DOI:10.14753/SE.2025.3192

SEMMELWEIS EGYETEM

DOKTORI ISKOLA

Ph.D. értekezések

3192.

TORDAI CSONGOR BALÁZS

Pszichiátria

című program

Programvezető: Dr. Réthelyi János, egyetemi tanár

Témavezetők: Dr. Réthelyi János, egyetemi tanár

Dr. Apáti Ágota, tudományos főmunkatárs

DOI:10.14753/SE.2025.3192

EXPLORING THE EFFECTS OF *DE NOVO* MUTATIONS IN SCHIZOPHRENIA USING INDUCED PLURIPOTENT STEM CELLS

PhD thesis

Tordai Csongor, MD

Semmelweis University Doctoral School

Mental Health Sciences Division

Supervisor: János Réthelyi, MD, Ph.D.

Ágota Apáti, D.Sc.

Official reviewers: Rita Padányi, Ph.D.

Krisztián Tárnok, Ph.D.

Head of the Complex Examination Committee: Miklós Geiszt, MD, D.Sc.

Members of the Complex Examination Committee: Karolina Pircs, Ph.D.

Judit Lazáry, MD, Ph.D.

Budapest

2025

DOI:10.14753/SE.2025.3192

Table of Contents

DOI:10.14753/SE.2025.3192

DOI:10.14753/SE.2025.3192

List of Abbreviations

hiPSC – Human Induced Pluripotent Stem Cell

SCZ – Schizophrenia

SNP- Single Nucleotide Polymorphism

SNV – Single Nucleotide Variation

CNV – Copy Number Variation

DNM – De Novo Mutation

GWAS – Genome Wide Association Study

lncRNAs - long non-coding RNAs

PRS - Polygenic Risk Score

hiPSC – human induced Pluripotent Stem Cell

CRISPR - Clustered Regularly Interspaced Short Palindromic Repeats

PBMCs - Peripheral Blood Mononuclear Cells

ZMYND11 - Zinc Finger MYND-Type Containing 11

KHSRP - K-Homology Splicing Regulatory Protein

LRRC7 - Leucine-Rich Repeat Containing 7

KIR2DL1 - Killer Cell Immunoglobulin-Like Receptor, Two Domains, Long Cytoplasmic Tail 1

PHD - Plant Homeo Domain

PWWP - Proline-Tryptophan-Tryptophan-Proline domain,

MYND - Myeloid, Nervy, and DEAF-1 domain

mRNA - messenger Ribonucleic Acid

miRNA – microRNA

DGGC - Dentate Gyrus Granule Cell

MEF - Mouse Embryonic Fibroblast

qPCR - quantitative Polymerase Chain Reaction

ICC – Immunocytochemistry

ULA - Ultra Low Attachment

EB - Embryoid Bodies

NHEJ – Non-Homologous End Joining

HDR – Homology Directed Repair

PAM - Protospacer Adjacent Motif

NPCs - Neural Progenitor Cells

ROI - Regions Of Interest

GO - Gene Ontology

DO – Disease Ontology

PCA - Principal Component Analysis

DE - Differential expression

OE – Overexpression

UE – Underexpression

DOI:10.14753/SE.2025.3192

ASD - Autism Spectrum Disorder

NLS - Nuclear Localization Signal

DOI:10.14753/SE.2025.3192

1 Introduction

I would like to provide some context about the setting in which this work was conducted. During my doctoral years, I was fortunate to have had two supervisors and to be part of two research groups that closely collaborated.

One group is the Molecular Psychiatry Research Group, led by János Réthelyi at the Semmelweis University Department of Psychiatry and Psychotherapy. From my perspective, János is primarily a psychiatrist driven by a deep interest in understanding disease pathomechanism and translating research findings into tangible benefits for patients. The central research question that motivates this group is: what happens at the biological level in the brain of a schizophrenia (SCZ) patient? More specifically, which genetic alterations are involved, and how do they cause disruptions at the cellular level?

The other group is the Human Pluripotent Stem Cell Laboratory, led by Ágota Apáti at the Institute of Molecular Life Sciences within the Hungarian Research Network Research Center for Natural Sciences (HUN-REN RCNS). From my perspective, Ágota is more focused on fundamental scientific questions, such as understanding how stem cells function and identifying the characteristics that enable them to perform their roles. Historically, this group has been at the forefront of using calcium imaging techniques and studying transport proteins in human pluripotent stem cells. With the expertise in culturing, editing, and differentiating human pluripotent stem cells, as well as proficiency with molecular biology tools, this lab was the ideal partner for the Molecular Psychiatry Research Group to collaborate with on hiPSC-based disease modeling projects.

1.1 Schizophrenia is a neurodevelopmental disorder with polygenic background and poorly understood pathogenesis

Schizophrenia (SCZ) is a chronic psychiatric disorder affecting approximately 1% of the global adult population (1). It is characterized by a range of symptoms including hallucinations, delusions, disorganized behavior and speech, i.e. positive symptoms, and decreased motivations, anhedonia, and social withdrawal, i.e. negative symptoms, moreover neurocognitive impairments (2, 3). These symptoms often lead to significant impairments in educational and occupational performance, as well as challenges in social functioning, despite the availability of pharmacological and psychosocial treatments.

Extensive research into the genetics and neurobiology of SCZ has uncovered various molecular mechanisms and brain alterations associated with the disorder (4). However, our understanding remains incomplete, and current therapies are insufficient. Novel approaches are needed to better characterize the biological underpinnings of SCZ.

Recently, the neurodevelopmental theory of SCZ has gained substantial interest (5). This theory posits that SCZ results from a complex interplay between genetic and environmental risk factors that influence early brain development, and the trajectory of biological adaptation to life experiences (6). This perspective underscores the importance of investigating the genetic and developmental origins of the disorder, to develop more effective clinical interventions.

1.1.1 Genetic risk of SCZ: the role of de novo mutations and rare variants.

It is well-established that SCZ is a polygenic disorder with high heritability (7-9). The genetic architecture of SCZ includes common genetic variants with small effects, such as single nucleotide polymorphisms (SNPs), and rare mutations with larger effects, such as single nucleotide variants (SNVs) and gene copy number variation (CNVs). SNPs are transmitted, while SNVs can be inherited or acquired during parental meiosis, i.e., *de novo* mutations (DNMs), which arise spontaneously from one generation to the next.

Disease causing DNMs are often localized in protein-coding regions. DNMs can have significant impacts on disease risk by perturbing essential molecular pathways in neurons (10). Investigating the degree of how much DNMs contribute to SCZ risk is challenging because large genome-wide association studies (GWAS) do not differentiate between inherited and *de novo* variants, and lack the resolution needed to identify rare variants (11).

The enrichment of rare variants in SCZ has been observed by exome sequencing across various ancestries in genes that are highly conserved evolutionarily, such as *SETD1A, CUL1, XPO7, TRIO, CACNA1G, SP4, RB1CC1,* and *AKAP11* (12). These genes are primarily involved in glutamatergic synapse formation and regulation, although other rare variants have also been reported (12, 13). The latest GWAS findings (14) also point to the involvement of synaptic genes in SCZ pathogenesis.

While exome sequencing for rare variants in protein-coding genes is not yet part of the clinical protocol for SCZ, it has been suggested that it could provide valuable insights into the etiology and treatment of individual patients (15). Attempts have been made to summarize the cumulative risk that SNPs can contribute to overall SCZ risk (16). Polygenic risk score (PRS) analysis was developed, that is a tool used to estimate an individual's genetic predisposition to developing SCZ. While PRS can help identify individuals at higher risk and improve early detection strategies, it is limited in its ability to predict outcomes at the individual level due to the complex interplay of genetic and environmental factors. Based on this, we considered it worthwhile to experimentally investigate rare genetic variations with larger effects, as these are more likely to reveal the biological impact caused by the mutation and the disease mechanism.

1.1.2 SCZ pathomechanism: Shifting from dopamine and the prefrontal cortex to hippocampal and glutamatergic factors.

The pathogenesis of SCZ involves multiple theories, including dopaminergic dysregulation, general synaptic dysfunction, neurodevelopmental alterations, and glutamatergic abnormalities (2). Different brain regions, particularly the prefrontal cortex and the hippocampus, play crucial roles in these processes.

Classically, the dopamine hypothesis suggested that enhanced presynaptic dopamine activity in the striatum primarily contributes to psychotic symptoms, while a decrease in dopaminergic activity in cortical regions leads to negative and cognitive symptoms (17). Although evidence supporting various aspects of this model has been inconsistent (18), dopamine dysregulation remains the central target for most currently applied SCZ treatments. Despite convincing evidence of the neurodevelopmental origins of psychosis, current pharmacological treatments are usually initiated only after clinical diagnosis and focus on antagonizing striatal dopamine receptors (D2 receptors). These treatments are only partially effective, have various side effects, fail to address negative and cognitive symptoms, and are not useful as preventive measures (19).

There is a strong need in SCZ research to broaden the focus to include other neurotransmitter systems for example glutamate, and other brain regions such as the hippocampus.

Neuroimaging studies have shown structural and functional abnormalities in the hippocampus of SCZ patients, such as volume reduction, shape anomalies, and increased metabolism in the CA1 and subiculum sub-regions of the anterior hippocampus (20, 21). These abnormalities suggest a common pathophysiological mechanism, possibly related to hippocampal hypermetabolism and atrophy.

It has been hypothesized that increased extracellular glutamate concentration and dysregulated glutamate neurotransmission, primarily NMDA-receptor hypofunction contribute to the observed hypermetabolism and atrophy in the hippocampus (22). Computational and animal models support this hypothesis, showing that neonatal brain injury in the ventral hippocampus can mimic SCZ-like symptoms (23).

1.2 Challenges and methodological approaches in SCZ research

What approaches can deepen our understanding of the biology of this disorder? Post-mortem histopathological studies have been conducted for over a century and have revealed important macroscopic and microscopic abnormalities (24). However, his type of evidence has specific limitations, e.g. it is not possible to discern the effect of medications from pathophysiological processes. Ideally, direct examination of the living human brain would provide the most insights.

Technologies such as functional magnetic resonance imaging (fMRI), positron emission tomography (PET), and electroencephalogram (EEG) enable studies in living subjects, offering topographical information about regions like the dorsolateral prefrontal cortex and hippocampus. However, their limited spatial and temporal resolution often fails to guide biochemical and cellular research effectively (25). Molecular biology methods provide sub-cellular resolution but are not applicable to *in vivo* human studies.

Animal models have been valuable for understanding SCZ, using methods to induce similar conditions and investigate associated biological mechanisms. However, it is uncertain whether these models replicate the internal experiences of SCZ in humans (26).

The advent of human induced pluripotent stem cells (hiPSCs) has opened new possibilities (27). Derived from reprogrammed somatic cells, hiPSCs can differentiate into any cell type, including neurons, offering patient-specific models for studying psychiatric disorders. These models allow for direct investigation of *de novo* mutations through isogenic cell lines, enabling precise comparisons of how these mutations affect neuronal development and function (28, 29).

Moreover, hiPSCs facilitate high-throughput screening of therapeutic agents and personalized medicine approaches, making them a powerful tool in understanding and treating SCZ (30). This research area, known as "hiPSC-based in vitro disease modeling," represents a transformative step toward uncovering the molecular and cellular underpinnings of SCZ.

1.3 Recent advances of hiPSC based in vitro disease modeling of SCZ

The field of hiPSC-based disease modeling in SCZ began with the seminal work of Brennand et al. (2011) (28), followed by numerous studies examining different aspects of SCZ-related in vitro phenotypes. These studies have reported decreased synaptic connectivity and plasticity in glutamatergic synapses, impaired Wnt signaling , increased oxidative stress, altered mitochondrial function (31), and, in some cases, accelerated differentiation (32-34). Although most studies used cortical differentiation protocols, some focused on hippocampal development and adult neurogenesis, revealing significant alterations (35).

The phenotypes identified by each study are depending on several factors including patient selection, sample collection, reprogramming method, and the differentiation protocol used. Certain studies have genetically characterized patients, while others choose subjects based on clinical phenotype (for example treatment resistant SCZ). Sample collection is most commonly from peripheral blood or skin biopsy or hair follicle cells but can be any somatic living cell of the body. Reprogramming methods range from integrating vectors to transient expression of Yamanaka factors. Differentiation protocols use either induced expression or small molecule substitution. Since all these factors can influence the outcome of each study, more harmonized guidelines and protocols will be needed in the future to enable better integration of the obtained results.

1.3.1 Differentiation protocol

One major decision in disease modeling studies is what type of neurons to produce. We know that several types of neurons play a role in the pathogenesis of SCZ, and they would all be worth studying (various excitatory and inhibitory cells in the cortex, dopaminergic cells, various cells in the hippocampus, etc.). However, developing and using a differentiation protocol is energy and time consuming, so we had to choose one.

In previous studies, most research groups have produced cortical neurons and dopaminergic neurons (36). The study of SCZ using any type of hippocampal cells has been attempted by only a few research groups previously (37, 38) and these studies did not involve genetically characterized patients.

There is evidence implicating a link between hippocampal dysfunction and SCZ. One theory proposed by Lieberman et al. (39) is that hippocampal dysfunction is caused by dysregulated glutamate neurotransmission leading to hyperactivity and excitotoxicity, eventually causing atrophy, particularly in the CA1 region.

Another idea linking SCZ to the hippocampal formation is that abnormal adult neurogenesis in the dentate gyrus, a special part of the hippocampus might be a potential cause of SCZ. This is based on clinical observations, postmortem, and functional imaging studies. Postmortem hippocampal samples from SCZ patients showed decreased expression of Ki-67, a cell proliferation marker (40). Moreover, smaller volume of the hippocampus in SCZ patients has been reported using meta-analysis of structural MRI studies (41). In addition to changes of cell proliferation, impaired maturation of adult-born dentate granule cells in patients with SCZ has also been reported (42). Interestingly, some studies have shown that clinical improvement was accompanied by the normalization of hippocampal size (43). Impaired adult hippocampal neurogenesis, as a distinct form of dysregulated neurodevelopment, might contribute to the structural changes and hippocampus-dependent affective and cognitive symptoms (44).

Based on this evidence, we decided to use a differentiation protocol that generates hippocampal dentate gyrus granule cells (DGGCs), a cell type crucial for adult neurogenesis in the hippocampus. The protocol was developed by Fred H. Gage’s

laboratory (37), and it is based on directed differentiation, by adding specific morphogens to the culture media in specific time windows of the differentiation process **(Figure 1)**.

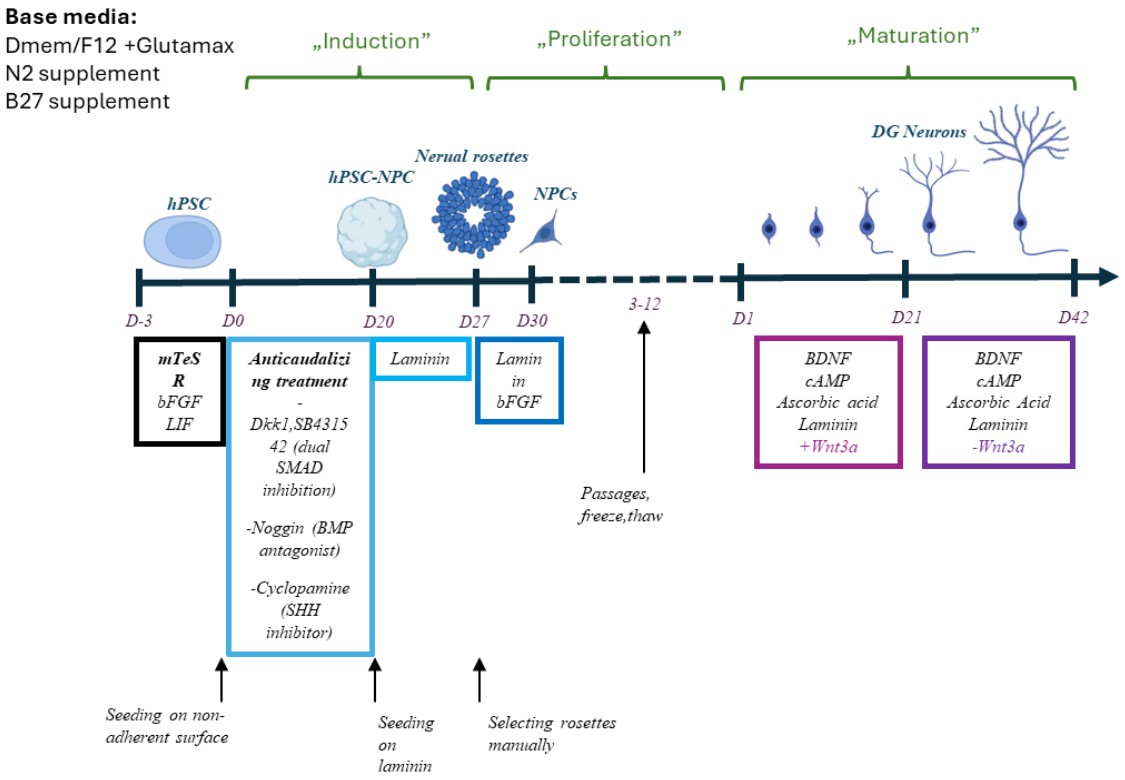

Figure 1. *Differentiation protocol used in the experiment to create hippocampal neural progenitor cells (NPCs) and dentate gyrus granule cells of the hippocampus. Directed differentiation was achieved by adding morphogens to the cell culture media. Surface of the culture dishes was coated by polyornithine-laminin. The protocol and figure were adapted from Yu et al. 2014 article (45).*

1.3.2 Limitations of hiPSC-based disease modeling

While hiPSC models provide valuable insights, they also have limitations. One critical question is how closely neurons differentiated from hiPSCs resemble *in vivo* differentiated neurons Notably, with current technology, it is only possible to produce cells resembling fetal neurons (46, 47). Modeling later stages of neuronal development *in vitro* remains a challenge.

Another difficulty with this method is the impact of unmonitored individual genetic variation on cellular phenotypes (48). Using case-parent trios to generate hiPSC lines

from the proband and both parents can be a good way to reduce these effects and simulate familial risk and the effects of specific DNMs. Another approach, CRISPR-editing (Clustered Regularly Interspaced Short Palindromic Repeats) cell lines to create isogenic copies of the patient cell line also reduces genetic heterogeneity (34, 49, 50).

Additionally, the complex genetic background of SCZ complicates efforts to form a unified hypothesis of its pathophysiology. Investigating the effects of specific, high-impact DNMs can help break down this complexity into more manageable pieces, similar to the successful use of hiPSCs in modeling monogenic diseases.

In my Ph.D. thesis, I present two research projects involving hiPSC-based disease modeling of SCZ. Our main objective in both cases was to understand the impact of DNMs on SCZ patients. In both projects, reprogramming of peripheral blood mononuclear cells (PBMCs) from the patient was performed, but different approaches were used to create control lines.

In the following chapter, I summarize the work carried out before I joined the research group, and which laid the foundation for my PhD projects.

1.4 Previous results

1.4.1 Exome sequencing study of 16 SCZ case-parent trios identifying DNMs

The first step carried out before my participation in the project started was to identify DNMs in SCZ patients. The Department of Psychiatry and Psychotherapy at Semmelweis University conducted a whole exome sequencing study of 16 SCZ patients and their parents in the framework of the SCHIZOBANK study. Using next generation exome sequencing and Sanger-sequencing as validation, they were able to identify 12 *de novo* mutations in 9 patients. Each identified DNM was unique. 5 patients carried 1 DNM, while 2 patients had 2 and one patient had 3 DNMs (51).

Based on their known biological function, or previous genetic findings, some of the genes containing DNMs were probably not associated with SCZ pathogenesis, but some other genes including *LRRC7, KHSRP*, *ZMYND11* and *ADAMTS9* could be associated with SCZ pathogenesis (52, 53).

Two cases were chosen to participate in the hiPSC-based in vitro disease modeling studies: the patient carrying a mutation of *ZMYND11* and another case with 3 DNMS, *KHSRP*, *LRRC7*, and *KIR2DL1*.

1.4.2 1495C > T, a nonsense *de novo* mutation of the *ZMYND11* gene

One of our studies focuses on a de novo *ZMYND11* mutation in a 26-year-old male SCZ patient, characterized by predominant positive symptoms and mild negative symptoms, without intellectual disability. Exome sequencing identified a 10:293374C > T mutation, which results in a premature stop codon (R399X) affecting the nuclear localization signal. This nonsense mutation was not present in the patient's parents, suggesting its *de novo* origin (34). The ZMYND11 protein contains several important domains, including the plant homeodomain (PHD) finger, bromodomain (BROMO), CCCH-type zinc finger motifs, proline-tryptophan-tryptophan-proline (PWWP) domain, and myeloid, Nervy, and DEAF-1 (MYND) domain. **Figure 2** illustrates these domains and the location of the nuclear localization signal, which is affected by the mutation.

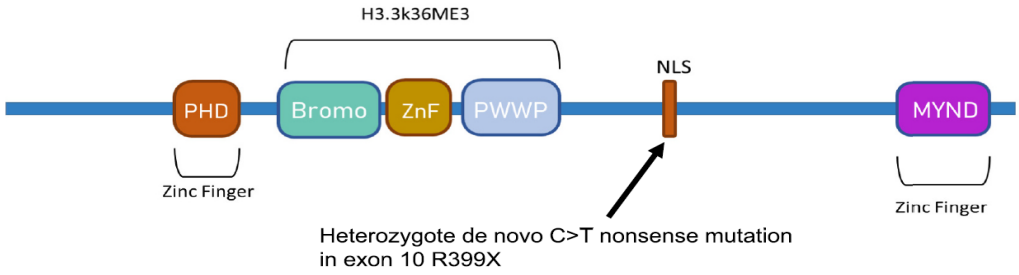

Figure 2. *Schematic diagram detailing the primary Zmynd11 domains: the plant homeodomain (PHD) finger, bromodomain (BROMO), CCCH-type zinc finger motifs, proline-tryptophan-tryptophan-proline (PWWP) domain, and myeloid, Nervy, and DEAF-1 (MYND) domain Additionally, the figure indicates the location of the nuclear localization signal (NLS). This depiction is adapted from Wang et al. (2014) (34, 54).*

Pathogenicity prediction algorithms, such as Varsome (55), rank this mutation as likely deleterious, as it disrupts an evolutionarily conserved region and affects 36 out of 39 alternative *ZMYND11* transcripts (**Table 1**).

Table 1. *Description of the identified DNM in the SCZ proband (34).*

Genomic position	10:293374C>T
Gene	*ZMYND11*
Variation type	nonsense
Amino acid change	R399X
Conservation of nucleotides	high
Conservation of amino acid	high
Varsome pathogenicity ranking	Likely pathogenic

The *ZMYND11* gene, also known as *BS69*, is located at chromosome 10p15.1 and consists of 15 exons. It is expressed in a variety of neuronal and non-neuronal cells, with the highest messenger ribonucleic acid (mRNA) levels in the thyroid gland, cerebellum, spinal cord, hippocampus, and frontal cortex (56). As a chromatin reader, *ZMYND11* binds the histone mark H3.3K36me3, acting as a transcriptional co-repressor and regulates mRNA maturation through intron retention (57). Mutations in *ZMYND11* have been linked to tumorigenesis, intellectual disability, epilepsy, and SCZ (15). However, the exact biological mechanisms behind these conditions remain unclear.

In neurons, *ZMYND11* functions as a repressor of neuronal differentiation, and its silencing accelerates this process (58).

Our hypothesis was that the truncated *ZMYND11* protein resulting in the 10:293374C>T nonsense mutation may not be able to enter the nucleus, impairing its function as a chromatin reader and transcriptional repressor. This would likely interfere with mRNA maturation, potentially contributing to the development of SCZ. To explore our hypothesis, my PhD work relied on hiPSC-based disease modeling to investigate the biological effects of this mutation in hiPSC derived progenitor cells and neurons.

1.4.3 *De Novo* Mutations of *LRRC7*, *KHSRP*, and *KIR2DL1* carried by a SCZ Patient

The second study I present investigates the effect of three DNMs in the genes LRRC7, KHSRP, and KIR2DL1, identified in a schizophrenia patient **(Figure 3).** This analysis also builds upon our previous exome sequencing and bioinformatics analyses.

DOI:10.14753/SE.2025.3192

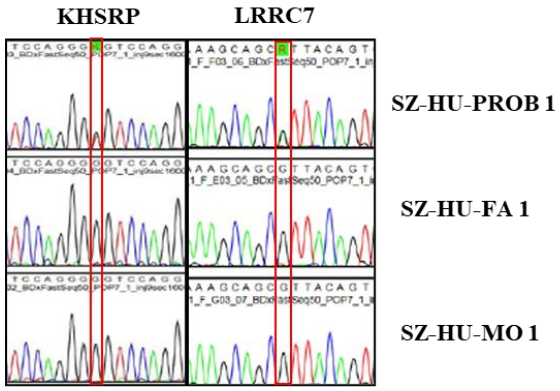

Figure 3. *Mutation of KHSRP and LRRC7 in SCZ patient. Sequencing results of hiPSCs derived from family members. Using the Sanger sequencing technique, we verified that the hiPSC lines from the trio members retained the original nucleotide sequences identified in the patient's mutations, confirming that only the patient was a heterozygous carrier of the missense variants (59).*

The *KHSRP* gene encodes the K-homology type splicing regulatory protein **(Figure 4),** an RNA-binding protein involved in multiple levels of RNA regulation, including mRNA decay, microRNA (miRNA) biogenesis, and interactions with long non-coding RNAs (lncRNAs) (60). *KHSRP* has critical roles in cell fate determination, immune response, neuronal differentiation, and neurite outgrowth (61). Its functions in neurons suggest it may play an etiologic role in neuropsychiatric disorders, including SCZ (62, 63). Indeed, *KHSRP* has been implicated as a potential SCZ risk gene in transcriptomic studies of circulating white blood cells (64).

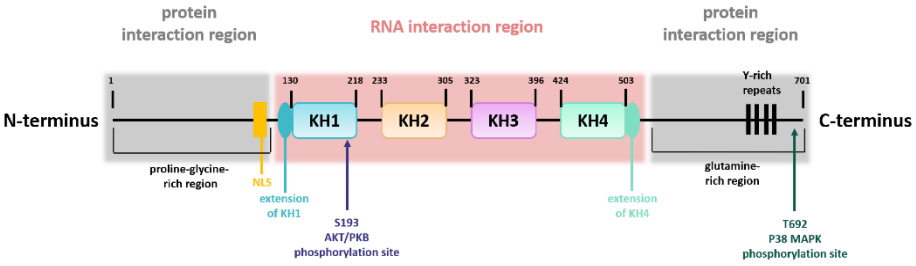

Figure 4. *Domain structure of the KHSRP protein (50).*

The *LRRC7* gene encodes densin-180, a postsynaptic density protein in glutamatergic synapses. In *LRRC7* knockout (KO) animal models, the loss of this protein led to decreased dendritic spine density and behavioral changes, including increased juvenile aggression, anxiety-like behavior, and social dysfunction in adulthood. These findings

suggest that *LRRC7* plays a role in emotional regulation and may contribute to neuropsychiatric disorders such as SCZ (65).

The *KIR2DL1* gene encodes a killer cell immunoglobulin-like receptor expressed by natural killer cells and some T cells (66). While important for immune regulation, this gene's mutation is unlikely to affect neuronal differentiation or function directly due to its tissue-specific expression, and therefore it was not investigated for further characterization in this study.

Our goal was to explore the biological effects of these DNMs using induced pluripotent stem cell (iPSC)-based disease modeling, applied to all members of a case-parent trio and an unrelated healthy control (**Table 2**).

Table 2. *Demographic and clinical data of the investigated case-parent trio, the extended family, and the codes of the hiPSC lines created from them (50).*

Subject	*Sex*	*Age*	*Medical History*	*Code*
Father	M	59	No psychiatric treatment or other major somatic disorders.	iPSC-SZ-HU-FA 1
Mother	F	55	No psychiatric treatment or other major somatic disorders.	iPSC-SZ-HU-MO 1 and 2
Proband (son)	M	24	Diagnosed with schizophrenia at the age of 17. During the past 10 years had 3 hospitalizations, receives clozapine treatment. Predominantly negative symptoms (measured by PANSS).	iPSC-SZ-HU-PROB 1 and 2
Unaffected older sibling	M	28	No psychiatric treatment or other major somatic disorders.	–
Younger sibling	F	21	Diagnosed with bipolar affective disorder at the age of 18 after a suicidal attempt. Receives lithium and olanzapine treatment.	–

After generating hiPSC by Sendai virus-based reprogramming and differentiating them into hippocampal dentate gyrus granule cells, we examined transcriptomic changes and tested specific cellular phenotypes associated with SCZ. We hypothesized that *KHSRP*

and *LRRC7* mutations would lead to transcriptomic and functional changes in hiPSC derived neurons.

The detailed description of the whole study is published in a research article listed as #3 in Bibliography of the candidate's publications and in the PhD dissertation of my colleague (50, 67). In the second part of my thesis, I present a summary of my contribution to the transcriptomic analysis and the results of the calcium imaging experiments. Our findings revealed significant transcriptomic alterations and subtle physiological changes in proband-derived neuronal progenitor cells.

1.4.4 Creation of a patient-derived hiPSC and isogenic control line

PBMCs obtained from the SCZ patient harboring the *ZMYND11* DNM were subjected to reprogramming via the Sendai virus approach, resulting in the establishment of a stable hiPSC line named Pat-Mut. The cells exhibited all the characteristic features of pluripotency (**Figure 5A and 5B**). OCT4 and NANOG are transcription factors essential for maintaining the pluripotent state, while SSEA4 is a surface antigen characteristic of undifferentiated pluripotent stem cells.

The cell line had a normal karyogram (**Figure 5D)** and was capable of spontaneously differentiating into all three germ layers (**Figure 5C)**, also characteristic of the pluripotent state.

These quality control experiments are important to confirm that the hiPSCs have retained their pluripotency, crucial for reliable differentiation into desired cell types for downstream analyses.

DOI:10.14753/SE.2025.3192

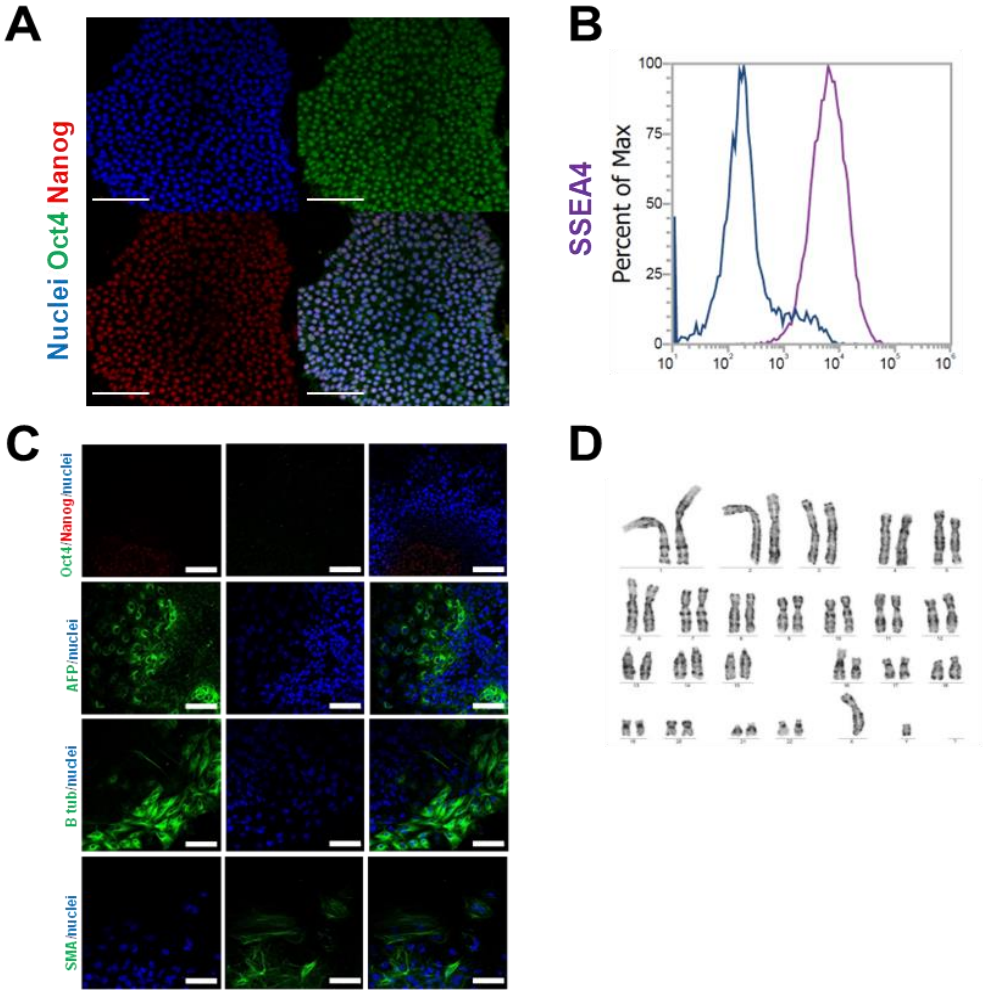

Figure 5. *Characterization of the schizophrenic patient derived (Pat-Mut) human induced pluripotent stem cell (hiPSC) line. A) Immunofluorescent staining reveals the expression levels of OCT4 (green) and NANOG (red) in undifferentiated cells. Scale bars are 100 µm. B) Flow cytometry analysis was employed to assess SSEA4 expression levels. Isotype control (blue) served as negative control. C) Immunocytochemistry (ICC) images of spontaneous differentiation of patient hiPSC cells; first panel showing absence of pluripotency markers OCT4 (green) and NANOG (red). On the second panel staining for endodermal marker AFP (green) is visible, third panel shows staining for ectodermal marker ß-III-tubulin (green), fourth panel shows staining for mesodermal marker SMA (green). The nuclei were counterstained by DAPI (2-(4-amidinophenyl)-1H -indole-6-carboxamidine - blue). Scale bars are 100 µm. D) Karyograms of chromosomes demonstrating normal male karyotype and no numerical chromosomal abnormalities for each sample (34).*

HiPSC lines were created from the *KHSRP* mutant patient and parent PBMCs with similar methodology and quality control. The codes for each cell line can be seen in **Table 2**.

1.4.5 Editing of hiPSCs by CRISPR to create isogenic control cell lines

To be able to investigate the biological consequences of the mutation, we needed similar or identical cells, which did not harbor the mutation. We decided to use CRISPR genome editing to create a genetically identical cell line also referred to as an isogenic cell, only differing in the corrected mutation. With the help of the endogenous repair mechanism called homology directed repair (HDR), the mutation was corrected (see details in the article Tordai et al 2024 (34)). The patient derived corrected cell line was named Pat-Wt.

Additionally, our goal was to introduce a mutation to a genetically independent healthy cell line that would replicate the effects of the patient-specific mutation in a different genetic background, allowing for a direct comparison of the functional consequences.

Non-homologous end joining (NHEJ) is a cellular process exploited in CRISPR genome editing to introduce mutations, because it efficiently repairs double-strand breaks without the need for a homologous template, often resulting in insertions or deletions that create frameshift mutations. In this study, NHEJ was employed to introduce a frameshift mutation at a specific site in the control cell line.

The original control line was named Ctrl-Wt, and the CRISPR edited cell line harboring the *ZMYND11* monoallelic mutation was named Ctrl-Mut (**Figure 6**). In this system, we can validate the differences between Pat-Mut and Pat-Wt by comparing Ctrl-Mut with Ctrl-Wt. If we see a similar change in the comparison of both isogenic lines, it is more likely that this change is the result of the *ZMYND11* mutation and not caused by individual clonal differences. In **Table 3** we summarize the names, genotypes, origin and editing of all the cell lines used in the experiments.

Table 3. *Description of CRISPR editing and genotype of the 4 hiPSC cell lines used in the in vitro experiments (34).*

Name	**Genetic background**	**Sex**	**CRISPR editing**	**ZMYND11 Genotype**
Pat-Mut	Patient-derived	male	-	+/-
Pat-Wt	Patient-derived	male	Correction of ZMYND11 mutation	+/+
Ctrl-Wt	Healthy control derived (XCL1)	male	-	+/+
Ctrl-Mut	Healthy control derived (XCL1)	male	Introduction of ZMYND11 mutation	+/-

DOI:10.14753/SE.2025.3192

Sanger sequencing of the CRISPR-edited hiPSC clones confirmed the correction of the point mutation in the patient-derived hiPSC line (**Figure 6A)** and the presence of the mutation in Ctrl-Mut cell line (**Figure 6B)**.

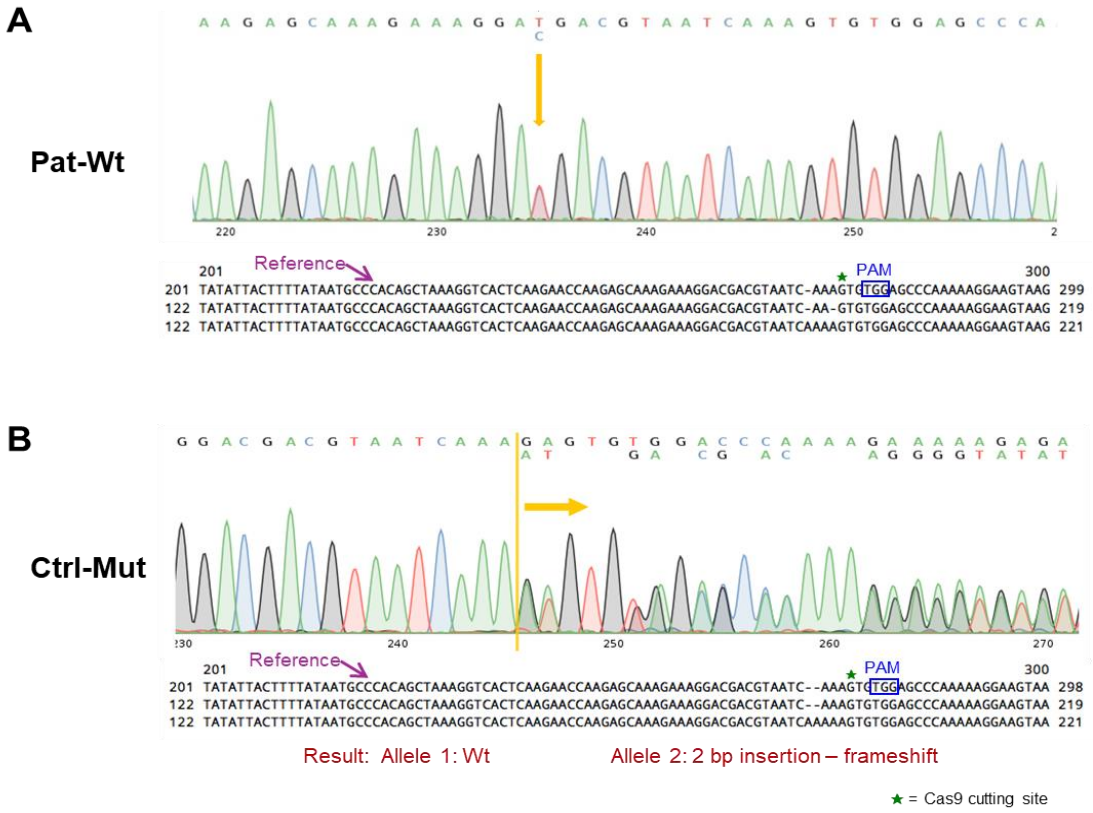

Figure 6. *Sanger sequencing data of CRISPR-edited hiPSC lines. A) A point mutation in the patient-derived clone is introduced indicated by the yellow arrow, correcting the originally present de novo mutation. B) Frameshift mutation in control (Ctrl-Wt/XCl-1) clone is highlighted by the yellow line and arrow. Additionally, the Cas9 cutting site is marked with a green asterisk, and the sequence is denoted in the reference sequence below the sequencing graphs (34).*

We conducted several experiments to confirm that genome editing did not change the pluripotent properties of hiPSC lines (**Figure 7**). The cells expressed SSEA4 surface antigen characteristic for pluripotent stem cells. (**Figure 7A**). The transcription factors OCT4 and NANOG demonstrated nuclear localization (**Figure 7B**). Investigation of 13–15 metaphase cells in all hiPSC lines revealed normal karyotypes (**Figure 7C**).

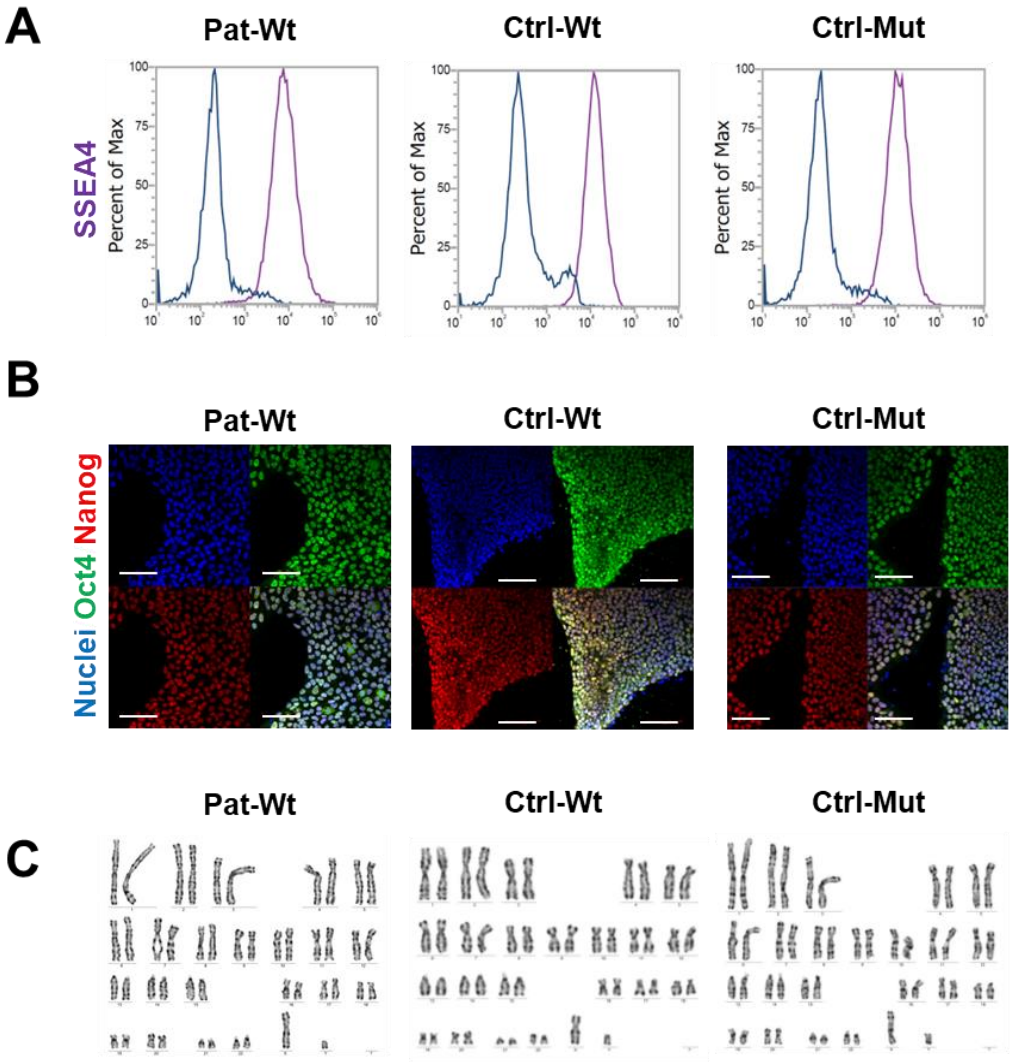

Figure 7. *Characterization of genome-edited hiPSC lines. A) Flow cytometry analysis was employed to assess SSEA4 expression levels (purple) in both wild-type (WT) cells and genome-edited clones. Isotype controls (blue) served as negative controls on each plot. B) Immunofluorescent staining reveals the expression levels of OCT4 (green) and NANOG (red) in undifferentiated cells, the nuclei were counterstained by DAPI. C) Karyograms of chromosomes demonstrating normal male karyotype and no numerical chromosomal abnormalities for each sample (34).*

1.5 Conclusion of the introduction

The investigation of DNMs in SCZ using hiPSCs and CRISPR-based genome editing provides a promising avenue for understanding the genetic and molecular underpinnings

DOI:10.14753/SE.2025.3192

of the disorder. By focusing on specific high-impact mutations, we can gain insights into the neurodevelopmental processes and synaptic functions disrupted in SCZ, contributing to better understanding of the disorder and the development of more targeted and effective treatments.

Before my participation in the studies, the patients carrying DNMs were selected from a cohort, the patient and isogenic control or parental control cell lines were created and established in the laboratory.

DOI:10.14753/SE.2025.3192

2 Objectives

The primary objective of this research was to investigate the biological effects of DNMs found in SCZ patients. We aimed to determine whether a given mutation plays a role in the development of SCZ in patients, to what extent, and through which mechanisms. Specifically, we seek to understand the molecular changes these mutations cause at the cellular level.

To address these broad questions, we formulated the following specific research objectives:

1. **Neuronal Differentiation of hiPSC lines from SCZ samples:**
   - Can pluripotent stem cells derived from SCZ patients develop into hippocampal neuronal progenitors and functional DGGCs?
   - Are there observable differences in the differentiation, growth and morphology of neural progenitor cells (NPCs) and neurons derived from SCZ patients?
2. **Analysis of transcriptomic profiles and protein expression of NPCs and neurons:**
   - Are there any changes in protein expression and transcriptomic profiles in SCZ samples compared to healthy and isogenic controls?
   - Does RNA sequencing reveal differences in mRNA profiles of NPCs and DGGCs derived from SCZ samples compared to their controls?
3. **Functional Assessment of NPCs and Neurons:**
   - Can NPCs respond to different external chemical stimuli, e.g. glutamate? Is this response different in SCZ samples compared to controls?
   - Do neurons derived from SCZ patients generate functional action potentials and calcium transients? Do they respond to the addition of neurotransmitters?
   - Is there a difference in the magnitude of the response?

3 Methods

3.1 Differentiation of hippocampal neural progenitor cells and dentate gyrus granule cells

NPCs were derived from the hiPSC lines Pat-wt, Pat-mut, Ctrl-wt, and Ctrl-mut, Proband, Mother and Father through embryoid body formation, following previously established protocols (Yu et al., 2014; Hathy et al., 2020). Rosettes were manually selected and dissociated with Accutase (Thermo Fisher Scientific, Waltham, USA) on day 27 or later, then re-plated onto new poly-ornithine/laminin-coated dishes in DMEM/F-12, GlutaMAX™ supplemented with N2/B27 medium, FGF2 (Thermo Fisher Scientific, Waltham, USA), and laminin. NPCs displayed consistent morphology after 5 passages and were utilized for experiments between passages p5 and p15.

For differentiation into DGCC neurons, NPCs were seeded onto poly-ornithine/laminin-coated plates in eight-well Nunc Lab-Tek II Chambered Cover glass with a density of $1.5x10^3$ cells, in N2/B27 medium supplemented with ascorbic acid, BDNF, cAMP, laminin, and Wnt3A. After 3 weeks, Wnt3A was removed from the medium, and the medium was refreshed every other day.

3.2 RNA sequencing

RNA sequencing was performed at both the hippocampal NPC and DGCC stages. Total RNA extraction was done using TRIzol™ reagent as per the manufacturer's guidelines (Thermo Fisher Scientific, MA, USA). Each cell line had three biological replicates. For NPCs, RNA was harvested from three different passages between p7-12 when they were approximately 70% confluent. Neurons were collected after 6 weeks of differentiation, starting from an initial seeding density of 24,000 cells/cm². The Illumina NovaSeq platform was utilized for NPCs (2x150 bp paired-end mode, yielding 36.5-55.3 million reads per sample), while the Illumina NextSeq system was used for neurons (1x75 bp single-end mode, producing 17.0-32.9 million reads per sample).

3.3 Immunocytochemistry

The characterization of hiPSC lines included testing the expression of transcription factors OCT4 and NANOG, as well as the surface marker SSEA4, using ICC and flow cytometry, respectively, according to established protocols (68). Immunofluorescence staining for NPCs and DGGCs targeting SOX2, Nestin, PROX1, and MAP2 was performed as previously described (50). ZMYND11 was immuno-stained using the BS69 antibody (Thermo Fisher Scientific, Waltham, USA, PA527899). Visualization was achieved with a Zeiss LSM 900 confocal laser scanning microscope and ZEN 3.1 software.

3.4 Calcium imaging and multi-electrode array measurements

Prior to all calcium imaging measurements, hippocampal NPCs were seeded for 2 days onto 8-well confocal chambers pre-coated with polyornithine/laminin and differentiated for 5 weeks. Cytoplasmic calcium signals were assessed using the Fluo-4 AM calcium indicator dye as previously described (50, 69). Baseline recordings were taken for 3–5 minutes before the application of 50 μM glutamate (Sigma, MO, USA). Cells were manually selected and marked as regions of interest (ROI) (100–300 per recording), and mean gray values were extracted using ImageJ. Cells with glial morphology were excluded from the analysis. The response was quantified by dividing the maximum fluorescence intensity post-application by the median fluorescence intensity of the baseline period for each cell. Statistical comparisons were conducted for each isogenic pair using the Mann-Whitney U test due to the non-normal distribution of single-cell reactions.

Extracellular electrophysiological recordings were performed using the MEA2100-System, controlled by the MEASuite software package (Multi Channel Systems MCS GmbH, Reutlingen, Germany) with a 10 kHz sampling rate. NPCs from each clone (3 biological replicates) were plated onto 60-6well MEA200/30iRTi polyornithine-coated chips, featuring six wells with nine 30 μm diameter titanium electrodes in each well. Neuronal differentiation followed the previously described protocol, and spontaneous activity was recorded after 5 weeks. Recordings were carried out at 37°C with a sampling

rate of 10 kHz. The raw recordings were filtered using a bandpass filter of 300-3000 Hz. Representative single electrodes were manually selected to demonstrate neuronal activity.

Spontaneous activity was defined by a custom made algorythm using Gaussian mixture model and random forest classification methods.

3.5 Statistical and data analysis

Data analysis was conducted using publicly accessible software tools and R packages. Initially, quality control of FASTQ files was conducted using FASTQC (FASTQC, 2023), followed by read alignment to the human reference genome (hg38) with hisat2 (70). Gene expression quantification was performed using FeatureCounts , and differential expression analysis was executed using the DESeq2 R package (version 1.36.0) (71) for each isogenic pair. Given the biological differences between the two RNA-seq experiments, batch correction was considered impractical due to the risk of masking significant biological changes between neurons and NPCs. Therefore, comparisons were restricted to isogenic pairs within each batch to maintain the inherent biological characteristics of the distinct cell types.

Following size factor normalization, a negative binomial distribution model was applied to compute statistical significance using a Wald test with Benjamini-Hochberg correction for multiple testing. Genes with fewer than 10 overall counts were excluded. Criteria for selecting differentially expressed genes included a log2 fold change (l2fc) > 1 or l2fc < -1 and an adjusted p-value < 0.05. To verify our findings and obtain an independent list of differentially expressed genes, a nonalignment-based pipeline using kallisto and sleuth was also employed. The hisat2-DESeq2 list was filtered using statistically significant results (qval < 0.05) from the kallisto-sleuth pipeline, without considering log2 fold change. Gene ontology (GO) and disease ontology (DO) analyses were performed using the ClusterProfiler R package (version 4.4.4), which uses a hypergeometric test to determine gene set and pathway enrichment. SynGO analysis was conducted using a publicly available online tool (72), and clustered heatmaps were generated with the "pheatmap" R package using default hierarchical clustering methods.

DOI:10.14753/SE.2025.3192

4 Results

4.1 Investigation of the effects of *ZMYND11* mutation

4.1.1 Morphological characterization and immunophenotyping of hiPSC-derived hippocampal NPC and DGGC cultures

To examine the potential cellular phenotype of the patient, we needed to generate neurons from pluripotent stem cells. We decided to implement a previously described directed neuronal differentiation protocol (37) that produces first hippocampal NPCs, and then DGGCs.

Neural progenitors were successfully derived from all four hiPSC lines (Pat-Wt, Pat-Mut, Ctrl-Wt, and Ctrl-Mut). The hippocampal NPCs exhibited similar morphology and growth characteristics across all cell lines (**Figure 8**).

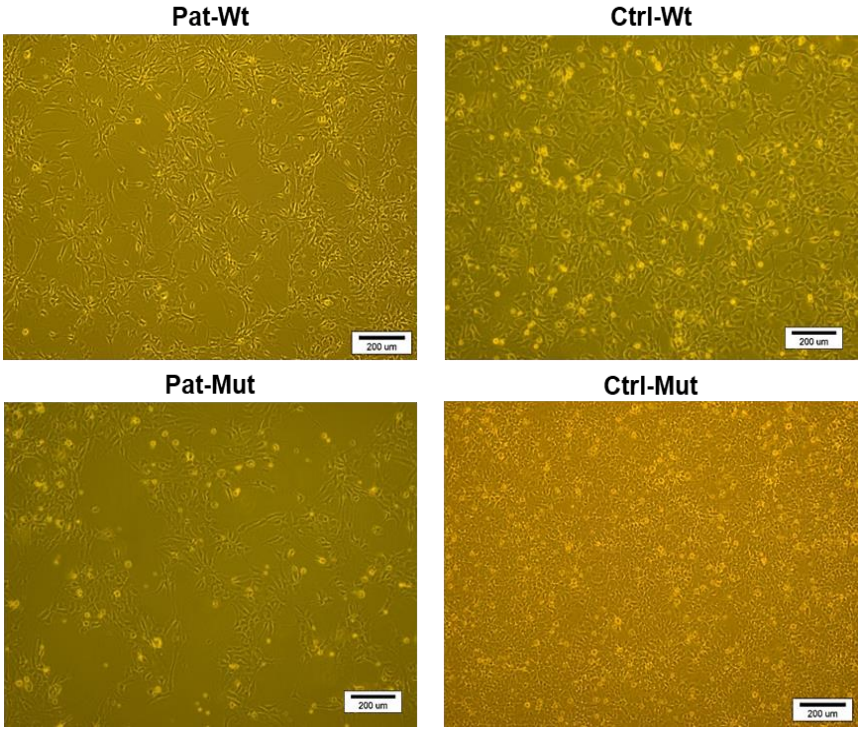

Figure 8. *Morphology of neural progenitor cultures. Phase contrast microscopy images of adherent hippocampal NPC cultures, before exposing the cells to Wnt3 containing differentiation media. Scale bars are 200 µm (34).*

DOI:10.14753/SE.2025.3192

All cell lines were expressing the neuronal progenitor markers Nestin and SOX2 (**Figure 9**).

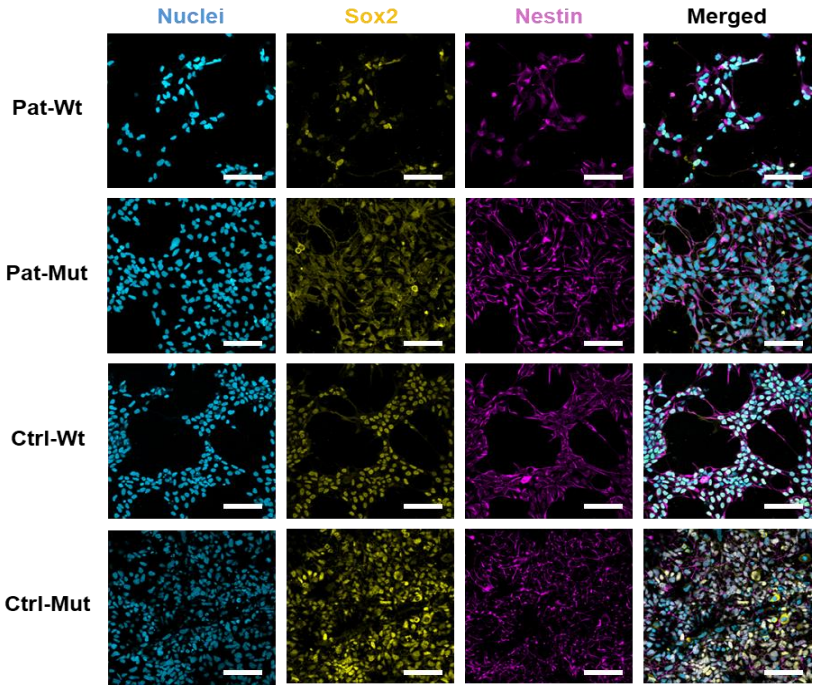

Figure 9. *Characterization of genome-edited human induced pluripotent stem cell (hiPSC)-derived hippocampal neural progenitor cells (NPCs). Representative images display immunofluorescence stainings of NPC cultures for NPC markers SOX2 (yellow) and Nestin (purple), conducted in at least two parallel experiments. Scale bars are 100 µm (34).*

DGCCs were differentiated from hippocampal NPC lines. (**Figure 10**).

DOI:10.14753/SE.2025.3192

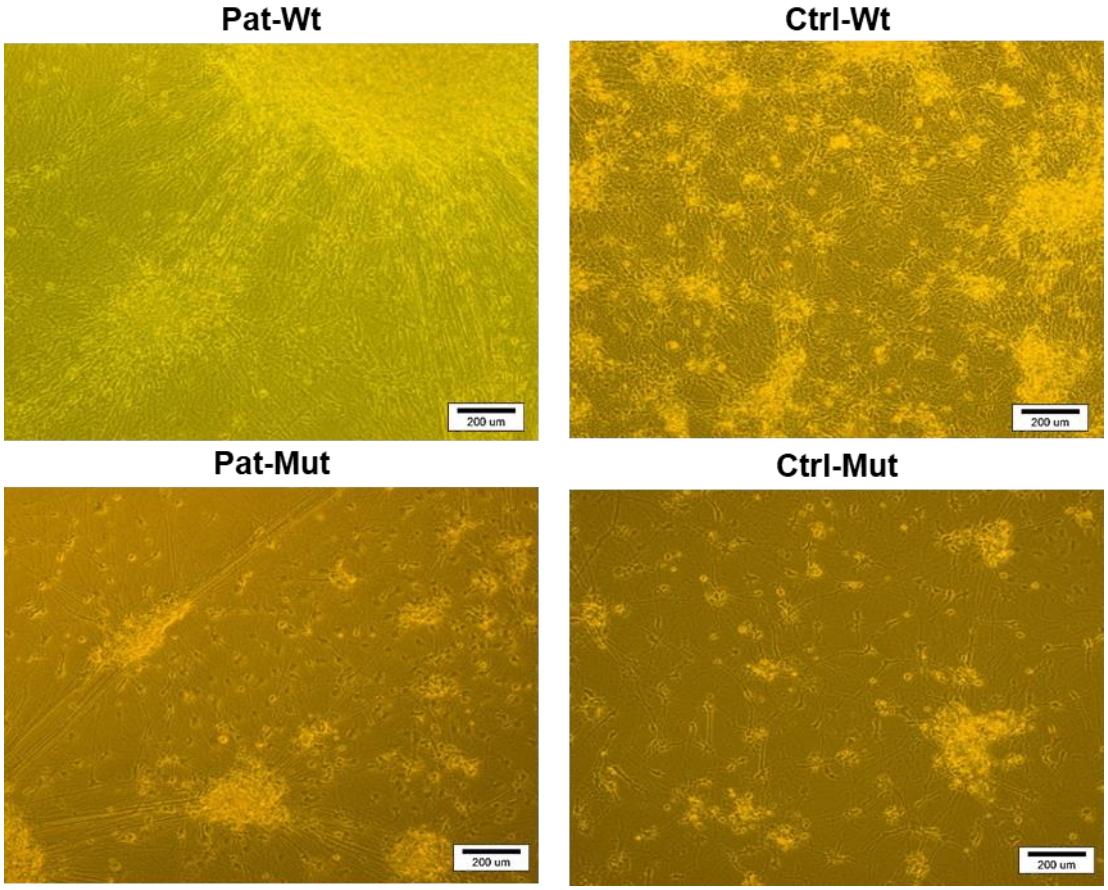

Figure 10. *Morphology of neural cultures. Phase contrast images of adherent hippocampal neuronal cultures on 6 well plates, at week 6 of differentiation.*

All samples showed PROX1 and MAP2 expression after 6 weeks of differentiation (**Figure 11**).

DOI:10.14753/SE.2025.3192

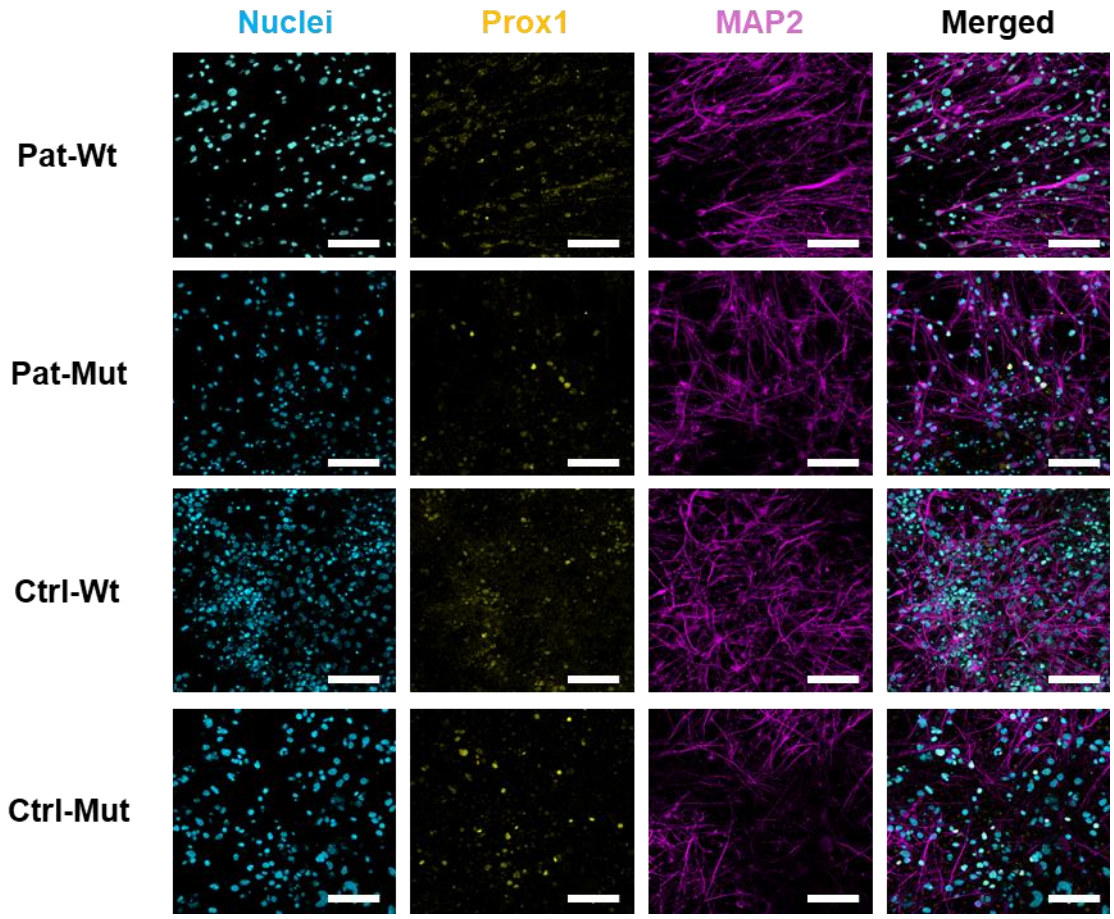

Figure 11. *Characterization of genome-edited hiPSC-derived neural cultures. Representative images demonstrate immunofluorescence staining for neural markers PROX1 (yellow) and MAP2 (purple) in neural cultures at 5 weeks of neural differentiation. Scale bars are 100 µm (34).*

4.1.2 Molecular properties: ZMYND11 localization in hiPSCs and during differentiation

When we examined the localization of ZMYND11 by ICC in hiPSC cells, we found that the nucleocytoplasmic ratio of the protein was changed in the mutant lines, with higher protein content in the cytoplasm than in the case of the control lines (**Figure 12**).

DOI:10.14753/SE.2025.3192

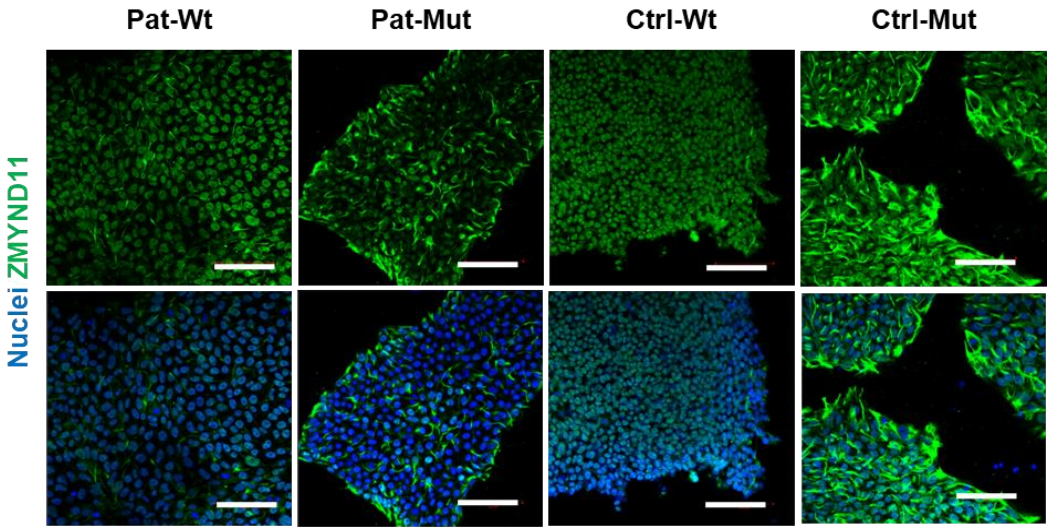

Figure 12. *Intracellular localization of ZMYND11 protein in hiCSs. Immunostaining was used to study the cellular localization of ZMYND11 (green). Mutant cell lines exhibit increased cytoplasmic and decreased nuclear staining. Nuclei were counterstained with DAPI (blue). Scale bars represent 100 µm (34).*

We further examined the localization of ZMYND11 during neuronal differentiation at the NPC stage and at the neuronal stage. Surprisingly, in all examined cell lines, the ZMYND11 protein predominantly localized in the cytoplasm and significantly accumulated in neurites, irrespective of genetic differences in NPCs (**Figure 13A)** and neurons (**Figure 13B**).

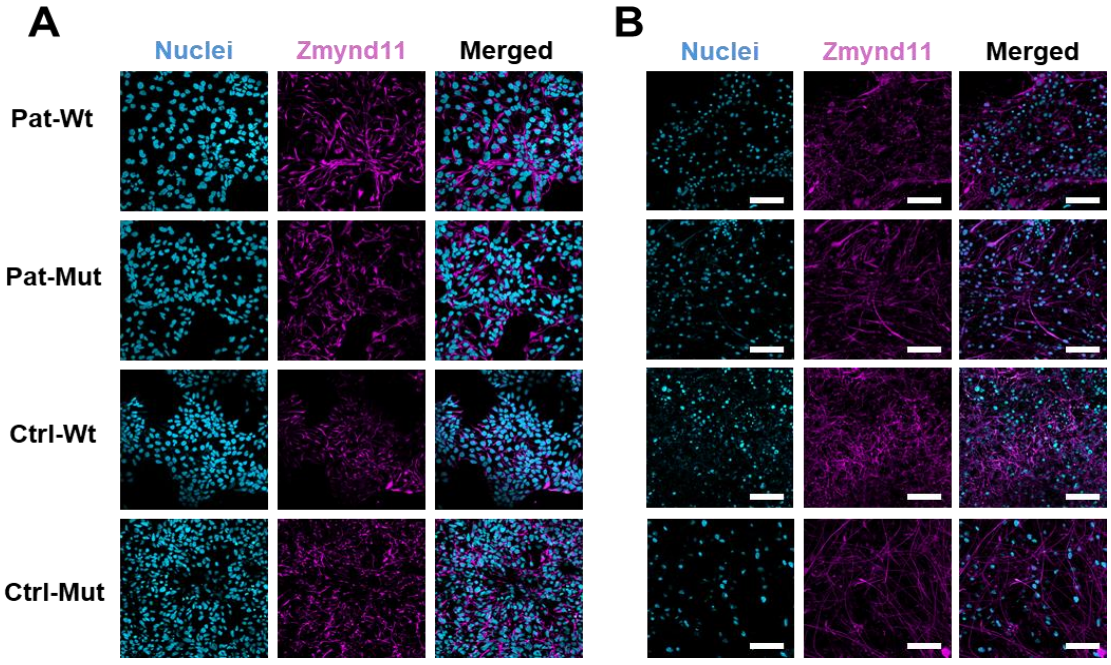

DOI:10.14753/SE.2025.3192

Figure 13. *Intracellular localization of ZMYND11 protein in NPCs (A) and neurons (B). Immunostaining was used to study the cellular localization of ZMYND11 (purple) during neuronal differentiation. The protein shows almost exclusively cytoplasmatic localization in all the studied cell lines. Nuclei were counterstained with DAPI (blue). Scale bars represent 100 μm (34).*

4.1.3 Transcriptomic Evaluation of Hippocampal NPCs and DGGCs

Bulk RNA sequencing was conducted on hippocampal NPCs and DGGCs to examine gene expression variations between *ZMYND11* mutant and wild-type cells and to identify crucial molecular pathways linked with the DNM. Faster interpretation of the result is supported by a symbol- and color-coded system, marking different genetic backgrounds and differentiation status (see in **Figure 14**).

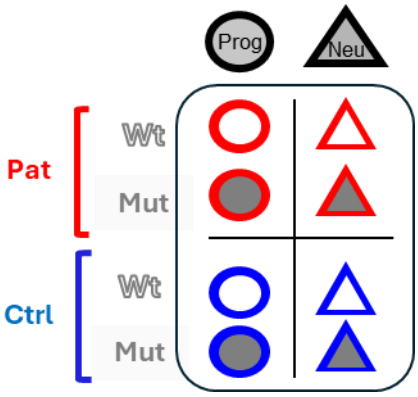

Figure 14. *Symbols used in further figures to give a visual aid in identifying the samples. Progenitors are marked with circles, while neurons are with triangles. Patient derived cell lines are marked with red edge, while control derived cell lines are marked with blue edge. ZMYND11 status is color coded by the center of the symbols: gray are mutant samples, while wild type samples are white centered.*

First, we examined the mRNA expression levels of ZMYND11 (**Figure 15**). We found that the *ZMYND11* mutation leads to reduced gene expression across both differentiation stages. The transition from progenitors to neurons is marked by a substantial increase in expression, indicating potential involvement of ZMYND11 in neuronal development.

DOI:10.14753/SE.2025.3192

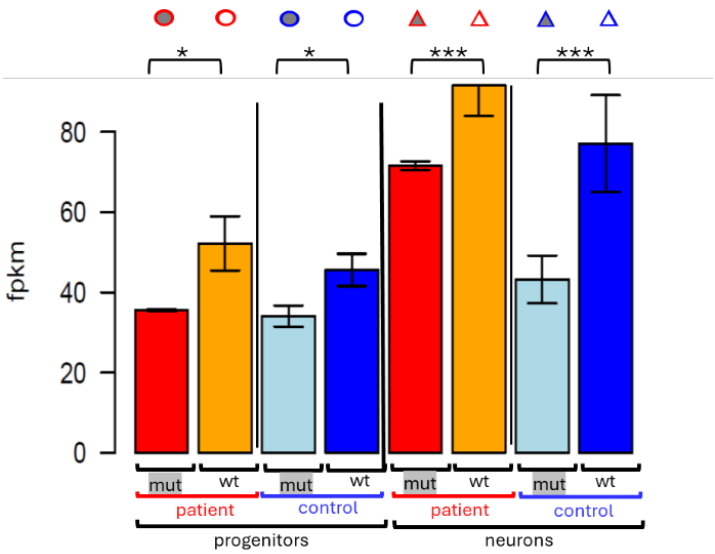

Figure 15. *ZMYND11 expression in neural cell types. Bar-plot showing the normalized read counts of ZMYND11 gene in all samples from RNA sequencing data. The vertical axis shows fragments per kilobase of million read values Heterozygous mutants have 20-40% decreased expression compared to wild types. The graph is based on the values of three biological replicates for each sample (34). Statistical analysis was done with DeSEQ2 tool in R, which uses Wald test with Benjamini-Hochberg correction. Pat-prog: mut vs. wt* p_{adj}*=0,043; Pat-neu: mut vs wt* p_{adj}*= 3.00E-06; Ctrl-prog. mut vs wt* p_{adj}*=0,044; Ctrl neu: mut vs wt* p_{adj}*=0.00016.*

Principal component analysis (PCA) including all the samples illustrates the significant impact of differentiation status, genetic background, and *ZMYND11* mutation on transcriptomic profiles in hippocampal NPCs and DGGCs (**Figure 16A**). There is clear separation between neurons and progenitors, accounting for the majority of variance (PC1 59,1%). Along the PC2 axis, which accounted for 13 % of the variance, samples were separated by genetic background into control- and patient-derived groups. Within each differentiation status, mutant and wild type samples are distinctly clustered, indicating the mutation's effect. When performing PCA only for NPCs, gene expression differences are primarily driven by mutation status and genetic background (**Figure 16B**), while in neurons we found similar patterns, though with less distinct separation (**Figure 16C**). Overall, these results demonstrate that the *ZMYND11* mutation significantly alters transcriptomic profiles.

DOI:10.14753/SE.2025.3192

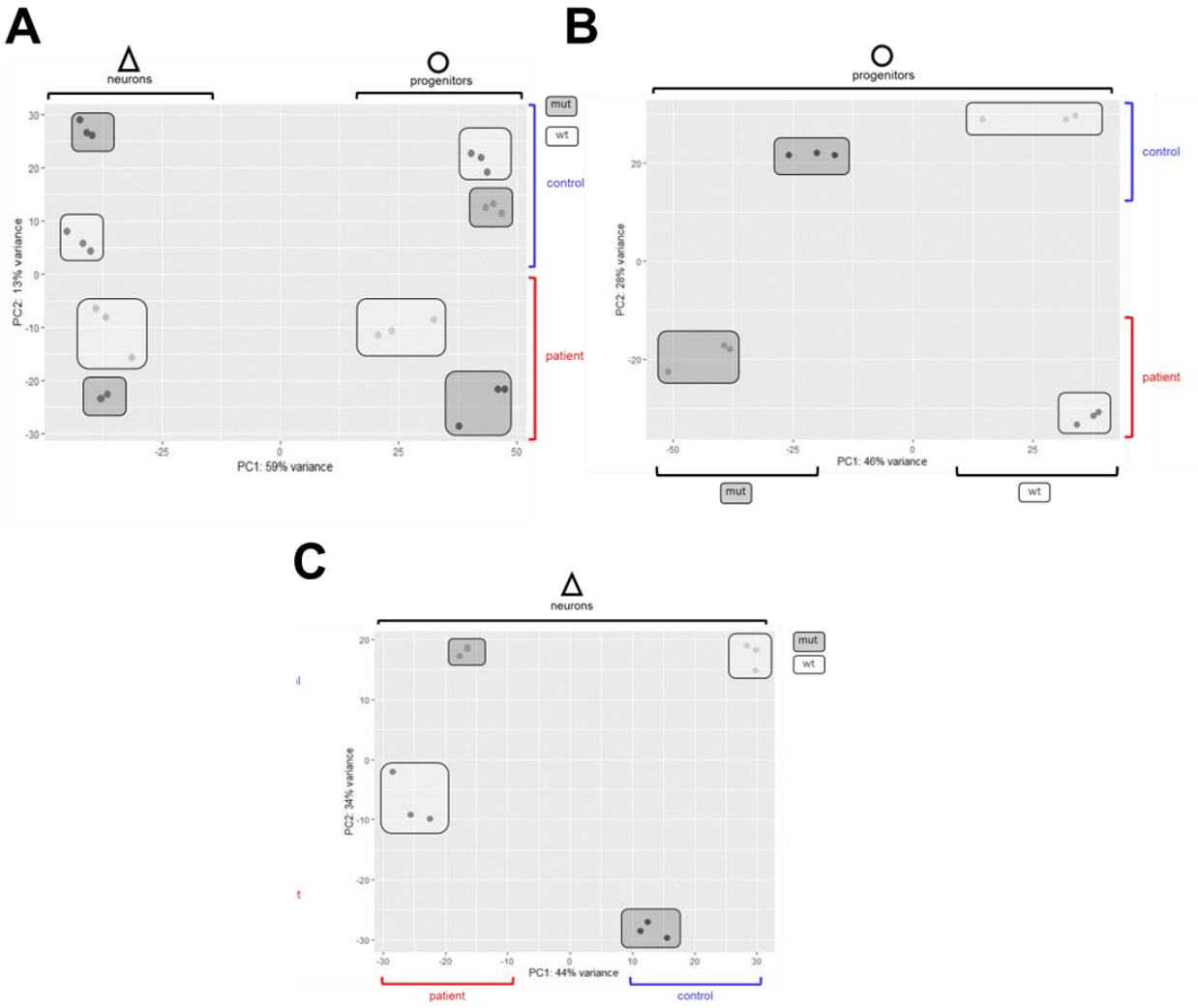

Figure 16. *Analysis of mRNA sequencing data in hippocampal NPCs and neurons. A) Principal Component Analysis (PCA) plot demonstrates the separation of samples based on their differentiation status and genetic background. B) PCA plot focusing on progenitor samples reveals separation based on ZMYND11 status (PC1) and genetic background (PC2). C) PCA plot focusing on neuron samples shows separation based on genetic background along the PC1 axis, with no separation based on ZMYND11 status along the PC2 axis (34).*

Differential expression (DE) analysis was complicated by three conditions creating variability of gene expression between samples: genetic background (Pat-Ctrl), developmental status (Progenitor-Neuron), and *ZMYND11* status (Mut-Wt). By having only progenitors in Experiment 1 and only neurons in Experiment 2, batch correction was not possible, as it would have erased the differences caused by neuronal development. We decided to first run DE analysis on all the isogenic pairs, comparing mutant to wild-

type cells in patient and control progenitors and neurons, respectively, resulting in four sets of DE genes, utilizing DESeq2 (**Figure 17A**). There were comparable numbers of DE genes in all four comparisons, ranging from 2660 to 3636.

The results were visualized using volcano plots to identify patterns of DE genes (**Figure 17B**). The ratio of upregulated to downregulated genes, and the extent of gene expression changes, as measured by log2Fold changes, were consistent across all comparisons. Genes with the highest log2Fold change and statistical significance varied between samples.

To obtain a more informative list of DE genes, first we used Sleuth, an independent DE analysis tool, to validate and filter the DESeq2 lists. Using 2 DE analysis tools allows for a more robust validation of the findings. Sleuth complements DESeq2 by offering a different statistical approach.

Then, to identify DE genes that were independent of genetic background, a list of DE genes common to both patient and control cell lines was compiled by intersecting the two sets, resulting in 580 common DE genes in progenitors and 202 common DE genes in neurons.

Further refining this list by intersecting the two sets resulted in a final list of 16 DE genes common to both progenitors and neurons (**Figure 17A and 17C**). This list includes *LHX1*, *LHX5*, *KHDRBS2*, *SHANK1*, and *ANO3* as overexpressed (OE) genes, and *CD74*, *FXYD5*, *RGCC*, *DNAJC15*, *BST2*, *CPNE8*, *ME3*, *SLC34A2*, *NABP1*, *ANXA2*, and *TPM2* as underexpressed (UE) genes (**Figure 17C**).

DOI:10.14753/SE.2025.3192

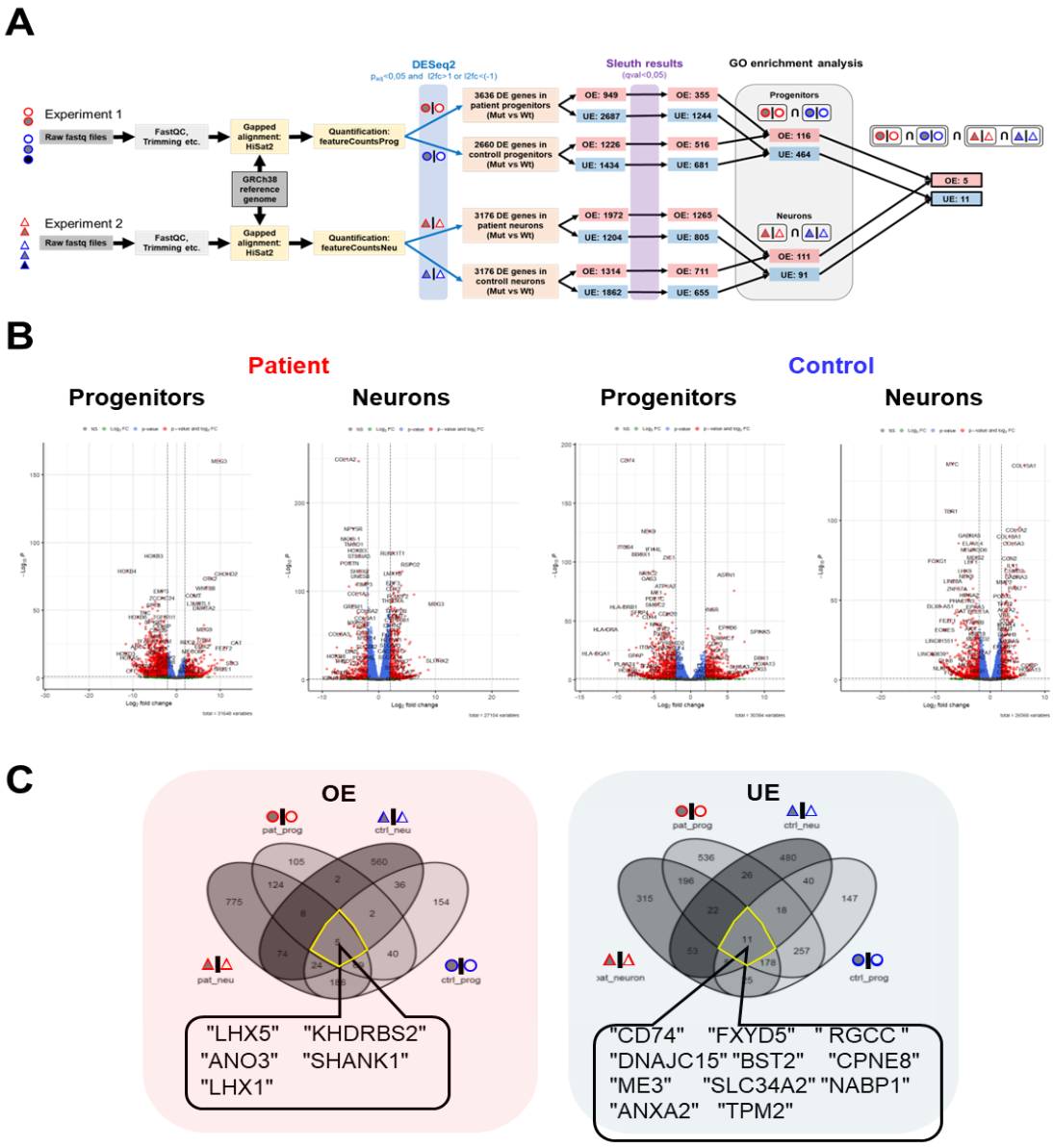

Figure 17. *Analysis of DE genes in NPCs and neurons A) Schematic representation of the analysis pipeline used to identify differentially expressed genes, resulting in five overexpressed and eleven underexpressed targets. This also highlights the gene sets utilized for Gene Ontology (GO) analysis B) Volcano-plots showing fold change and statistical significance of DE genes comparing mutant and wild-type samples, illustrating cut-off values for list-generation. There was similar amount of DE genes in all samples C) Venn diagrams depict the overlap of differentially expressed genes in patient and control progenitors and neurons. Genes from the innermost intersections, differentially expressed in both genetic backgrounds and differentiation phases, are indicated in chat boxes (34).*

DOI:10.14753/SE.2025.3192

Gene ontology (GO) enrichment analysis was conducted separately for NPCs and neurons from the common DE genes in both genetic backgrounds, specifically 580 DE genes for NPCs and 202 DE genes for neurons, as indicated in **Figure 17A** by the gray frame. This analysis revealed enriched terms related to neuronal function and development among OE genes, and terms related to extracellular matrix, cell adhesion, and glial function in UE genes (**Figure 18**). Enrichment analysis using the Disease Ontology (DO) database showed significant enrichment of genes involved in "developmental disorder of mental health" among OE genes in mutant neurons.

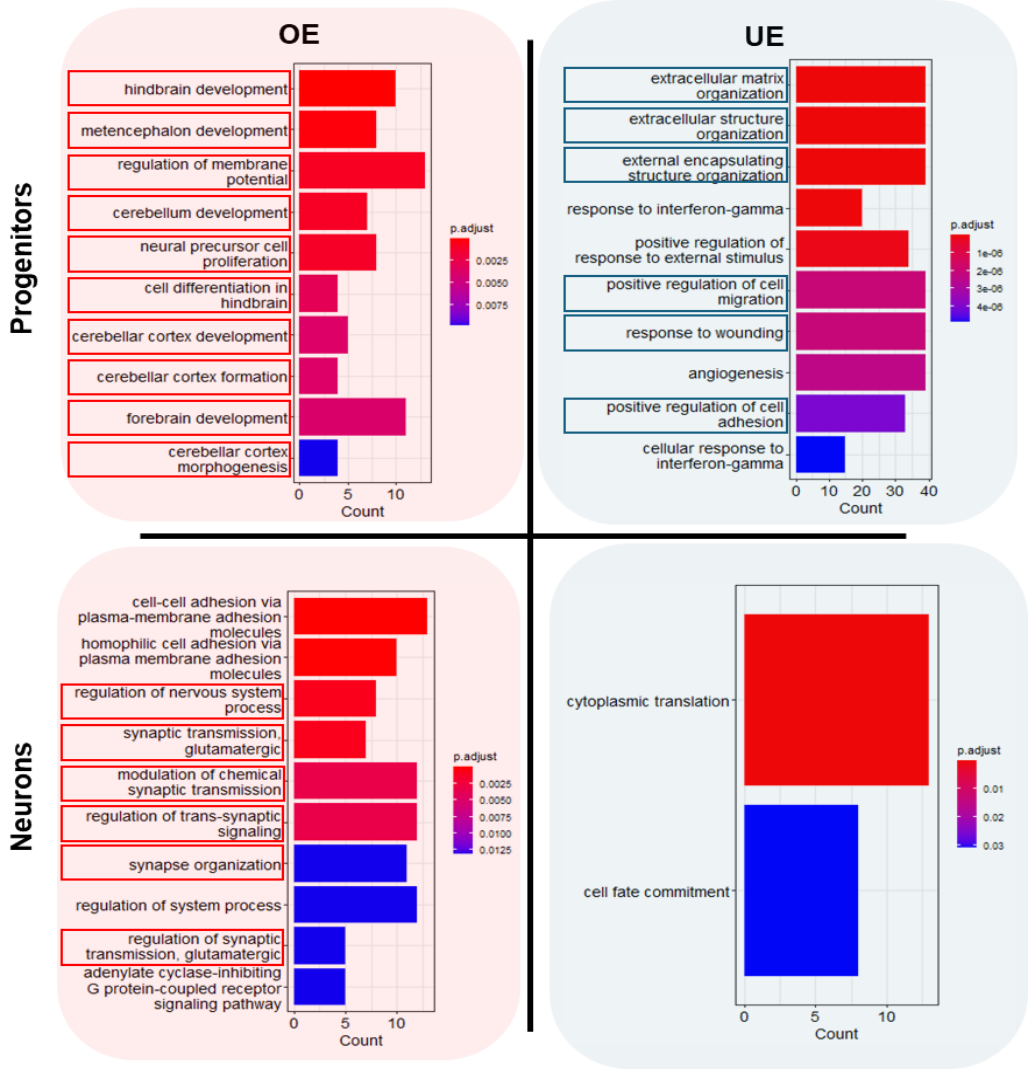

Figure 18. *Gene Ontology analysis of NPCs and neurons. Bar plots present the results of Gene Ontology Enrichment Analysis, with enriched categories on the vertical axis and gene counts for each category on the horizontal axis. Each bar is color-coded based on statistical significance for enrichment (34).*

Based on the enriched GO term "Synaptic transmission glutamatergic," further examination of glutamatergic receptor expression revealed higher levels in the mutant cell line compared to the wild-type cell line in both genetic backgrounds (**Figure 19A**). This pattern was less evident when investigating other neurotransmitter receptors.

Additionally, SynGO analysis was performed on the neuronal results (**Figure 19B**) to identify enriched gene sets associated with synaptic function. This analysis found enrichment of DE genes associated with the postsynaptic membrane in OE genes and enrichment of DE genes associated with post and presynaptic ribosomes among UE genes.

To visualize and integrate these results, we used PathView analysis online tool (73) (**Figure 19C**). On the virtual schematic representation of the glutamatergic synapse, it is visible that mainly the metabolic glutamatergic receptor pathway has significantly increased expression in the mutant neurons.

DOI:10.14753/SE.2025.3192

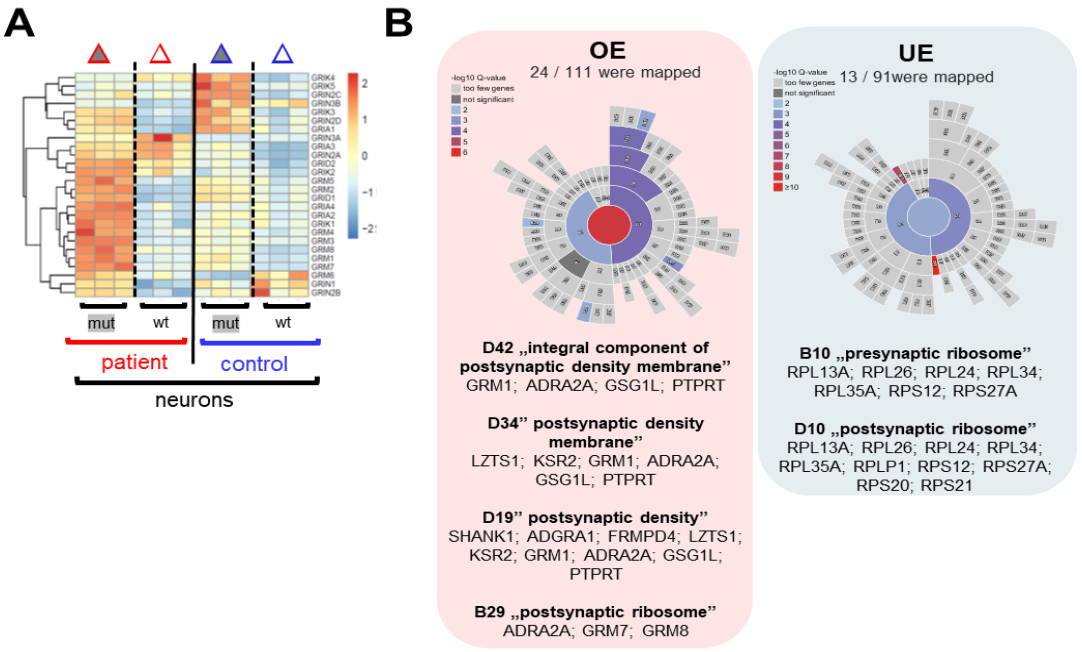

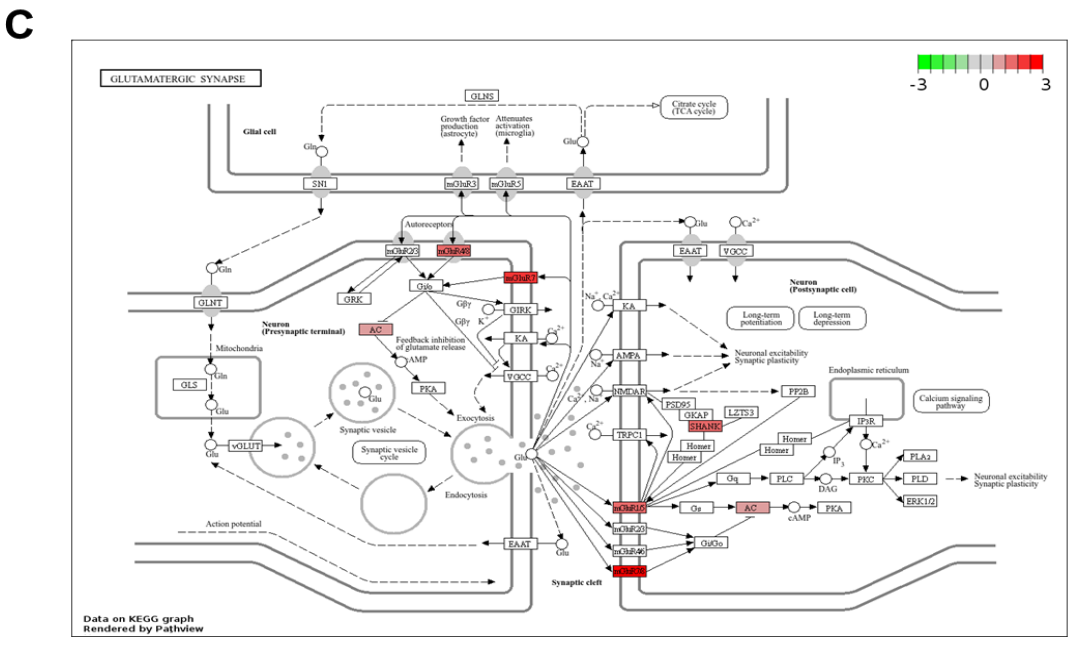

Figure 19. *Analysis of genes related to synaptic transmission. A) A clustered heatmap displays the relative expressions of glutamate receptor genes across neuronal samples, with expression values normalized row-wise. B) Synaptic genes were analyzed for Gene Ontology (GO) enrichment using the SynGO Database. "Sunburst" plots illustrate "cellular component" (CC) GO categories, with statistical significance for enrichment in our dataset indicated by color-coding. Mutant cell lines in both genetic backgrounds exhibit higher expression of most receptors compared to their isogenic controls. C) Pathway analysis of DE genes involved in glutamatergic transmission. A detailed schematic representation of the glutamatergic synapse,*

illustrating signaling pathways and interactions between cellular components involved in glutamate neurotransmission. DE genes are color-coded by the Log2FoldChange value in the mutant compared to the wild-type cells (34).

In summary, our results suggest that the heterozygous *ZMYND11* mutation significantly alters the transcriptome of developing NPCs and DGGCs. The upregulation of neural differentiation and functional genes may indicate precocious or accelerated differentiation, leading to an altered cellular phenotype. Furthermore, the involvement of synaptic machinery and glutamatergic receptor genes highlights the potential synaptic dysfunction in SCZ.

4.1.4 Functional measurements

The following experiments were conducted to elucidate the impact of transcriptomic changes on cellular behavior. By examining the physiological responses of the derived neural cells, we aimed to establish a clearer connection between the genotype and their phenotypic manifestations.

4.1.4.1 Multi-electrode array measurements

We were also able to grow each cell line on multi-electrode array surfaces that are suitable for detection of network wide electric activity of neurons by measuring uV-scale changes in extracellular field potential (**Figure 20A)**. All neuronal cultures exhibited spontaneous electrical potentials, such as spikes and bursting activity. (**Figure 20B**). This indicates the presence of functionally active synapses and action potentials in the neurons. Quantification and comparison of the detected signals between genotypes is currently in progress.

DOI:10.14753/SE.2025.3192

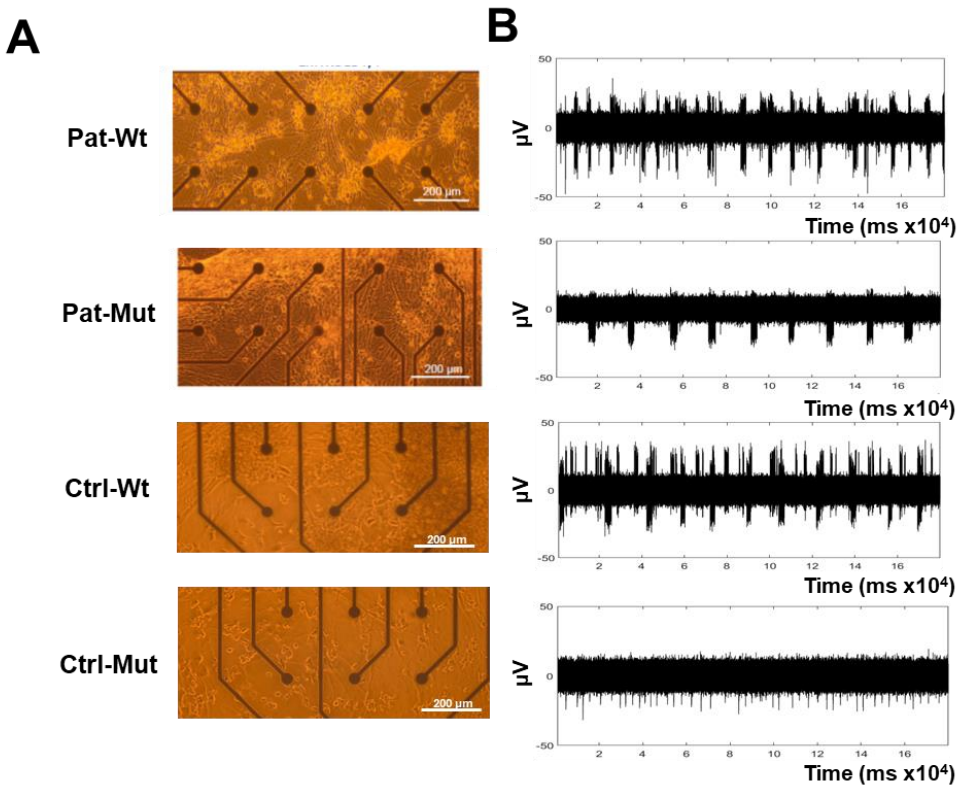

Figure 20. *Spontaneous electric and Ca-signals in neurons**.** A) Phase contrast images of hippocampal neuronal cultures on multi-electrode array chips, at 6 weeks of differentiation. Scale bars are 200 µm (34). B) Representative single electrode recordings from 3-minute multi-electrode array measurements exhibit signals indicative of neuronal activity. Functional assays demonstrate spontaneous calcium-transients and synchronized electrical activity detectable with multi-electrode arrays in all neuronal cultures between 4 and 6 weeks of differentiation (34).*

4.1.4.2 Calcium imaging: spontaneous activity and DGGC reaction to glutamate

Our other method of choice was calcium imaging given the crucial role intracellular calcium signaling plays in neurons: it regulates essential functions, including neurotransmitter release, gene expression, and synaptic plasticity, by acting as a secondary messenger. Additionally, from the technical aspect, calcium imaging allows real-time measurements, provides single-cell resolution within a cell culture, and many parameters are quantifiable, such as peak amplitude and frequency of spontaneous activity. It enables the parallel measurement of all the cells of a certain area of the cell culture and allows for repeated measurements.

DOI:10.14753/SE.2025.3192

Given these characteristics of calcium imaging, we may directly observe how transcriptomic alterations between mutant and wild type cells could influence neuronal function, providing a link between the genetic mutations and their phenotypic manifestations in neuronal activity.

Out of the many possibilities that calcium imaging allows, based on the transcriptomic results and literature search, we decided to assess the baseline spontaneous activity of DGGCs, and their reactivity to glutamate administration. During baseline measurements spontaneous calcium transients were detected and quantified. (**Figure 21A**). We observed relatively high variance of spontaneous activity between biological parallels of the same cell line. We could see differences between wild type and mutant cells, but these were not statistically significant, and the tendencies were not aligned with genotype differences in the different genetic backgrounds (**Figure 21B**).

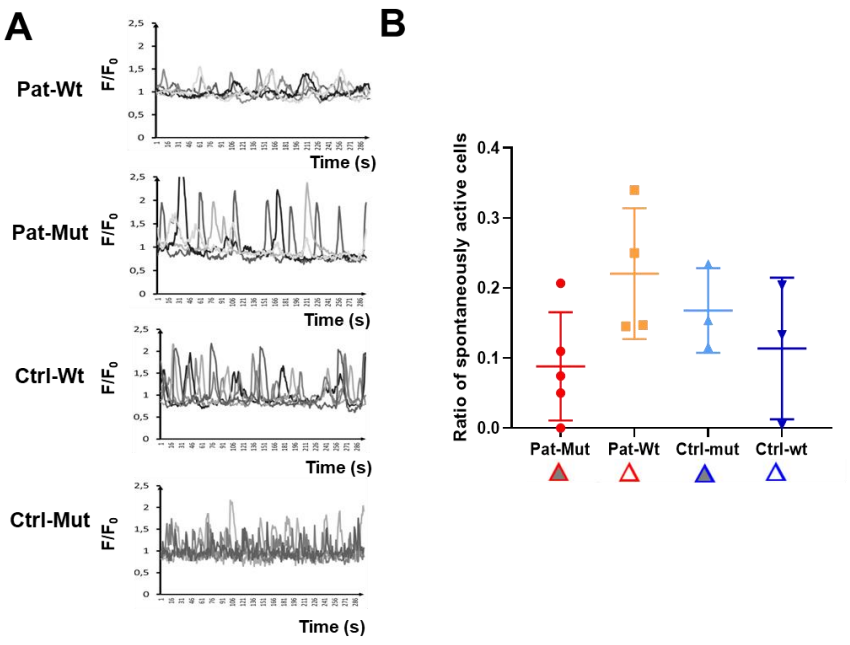

Figure 21 *Spontaneous calcium transients of DGGCs A) Examples of spontaneous Ca-transients in neurons are displayed, with five manually selected cells exhibiting spontaneous activity plotted per sample during a 5-minute measurement. B) Cells showing spontaneous calcium transients during the baseline recording divided by all the detected cells in one measurement. Spontaneous activity was determined by a custom-made algorithm described in methods section. No significant difference was found between genotypes. (Mann-Whitney test Pat-Mut vs Pat-Wt p=0.063, Ctrl-Mut vs Ctrl-Wt p=0.7) (34).*

After recording the baseline, we applied glutamate to the culture medium, and almost all the neurons exhibited an immediate increase in intracellular calcium concentration in both mutant and wild-type cultures (**Figure 22A and 22B**). Following an initial peak reaction, the intracellular calcium concentration remained elevated above the baseline until the end of the experiment (**Figure 22C**). Quantitative analysis from multiple experiments showed a significantly reduced reaction in the mutant cell lines compared to their wild-type counterparts. (**Figure 22D**).

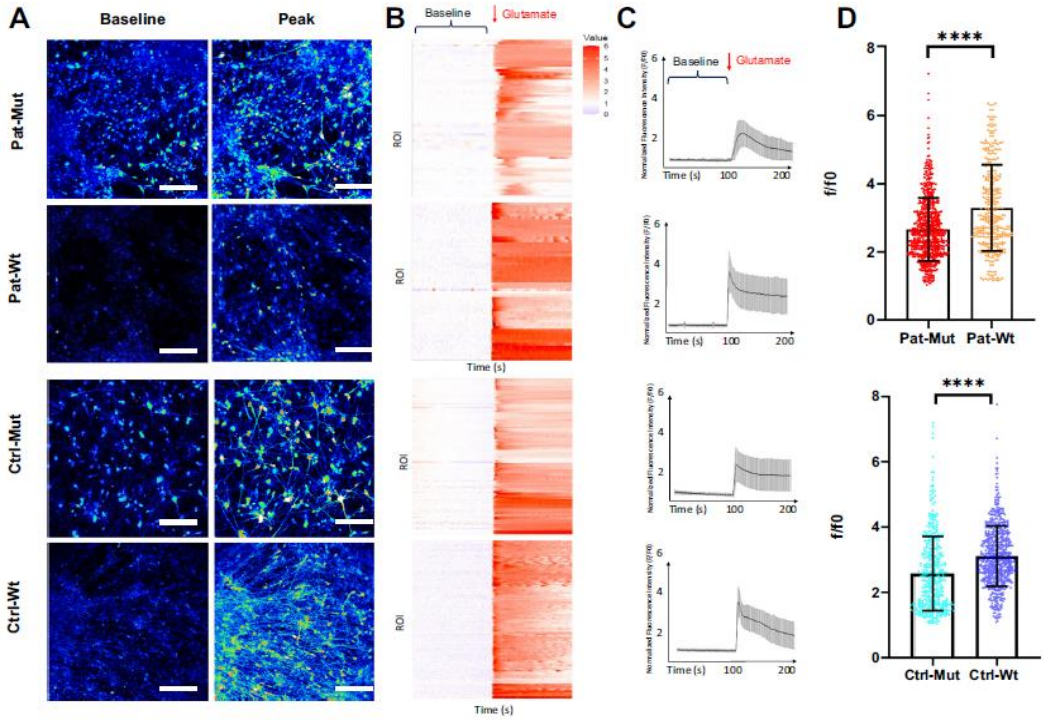

Figure 22 *Demonstration of calcium-imaging analysis of the response to glutamate in dentate gyrus granule cell cultures. A) Confocal microscopy images show neural cultures stained with Fluo-4-AM calcium dye, displaying baseline fluorescence and peak signal intensity. Scale bars: 100 μm. B) Heatmaps illustrate fluorescence intensity changes over time for regions of interest (ROIs).C) Average normalized fluorescence intensity (F/F0) during recording. D) Quantification of glutamate reaction involves 400–600 cells from 3 to 5 experiments, with a significant difference indicated by Mann-Whitney U test ($p < 0.0001$) (34).*

4.2 Investigation of the effects of *KHSRP* mutation

In the previous part of this thesis, I presented results from experiments involving the *ZMYND11* mutation, where we established a potential link between a DNM and subsequent disruptions in neurodevelopmental processes.

Next, I will present results from a project involving a different SCZ patient and a different methodological approach. Our observations in this case can lend support to our previously described findings.

This series of experiments focuses on hippocampal NPCs derived from a patient carrying DNMs in the *KHSRP* and *LRRC7* genes. *KHSRP* is a multifunctional RNA-binding protein implicated in various neuronal processes, including alternative splicing and mRNA localization (for more details see the Introduction). In this investigation, we generated hiPSCs using Sendai virus vectors from the patient and compared them to those from unaffected family members (59).

The establishment, characterization and differentiation of the cell lines are described in detail in the thesis of my colleague, Edit Hathy (67). Here I would like to summarize the findings of the transcriptomic analysis and then show the result of calcium imaging experiments in detail.

4.2.1 Transcriptomic differences in KHSRP and LRRC7 mutant NPCs

At the NPC stage, bulk RNA sequencing analyses identified transcriptional differences linked to KHSRP and LRRC7 mutation. Differentially expressed (DE) genes were determined in the SCZ patient line compared to both the father and mother lines (**Table 2**). GO and PATHWAY analyses showed enrichment of DE genes in pathways related to neuron formation, axon development, neurogenesis, Wnt signaling, and Calcium signaling. Among the 100 examined DE genes, many were transcription factors and neuron specific. Several DE genes were KHSRP target genes, i.e., genes regulated by KHSRP, such as *ERBB4*, *GRIN2A*, and *KHDRBS2*, may contribute to SCZ etiology.

For more details see Edit Harthy's doctoral thesis (67) or Hathy et al. 2020 (74).

4.2.2 Functional phenotypes found in the *KHSRP* mutant by Calcium imaging

Since the transcriptional differences indicated synaptic genes, following the same approach as before, we investigated the functional activity of NPCs derived from the case-parent trio using Calcium imaging techniques.

We recorded and analyzed both their spontaneous activity and glutamate-induced activity. Similar to our group's previous findings (75), the NPCs showed low levels of spontaneous activity but responded to glutamate stimulation with characteristic patterns (75). Using the ANCOVA model, we observed significant differences among the subjects ($F = 286.78$, $p < 0.001$). Specifically, each NPC culture significantly differed from one another after adjusting for the covariate ($F = 837.62$, $p < 0.001$). The NPCs derived from the SCZ patient showed a significantly different, weaker response to glutamate compared to the others. The mother NPCs exhibited the strongest glutamate response (Ca NPC-SZ-HU PROB < Ca NPC-SZ-HU-FA < Ca NPC-SZ-HU-MO, **Figure 23**).

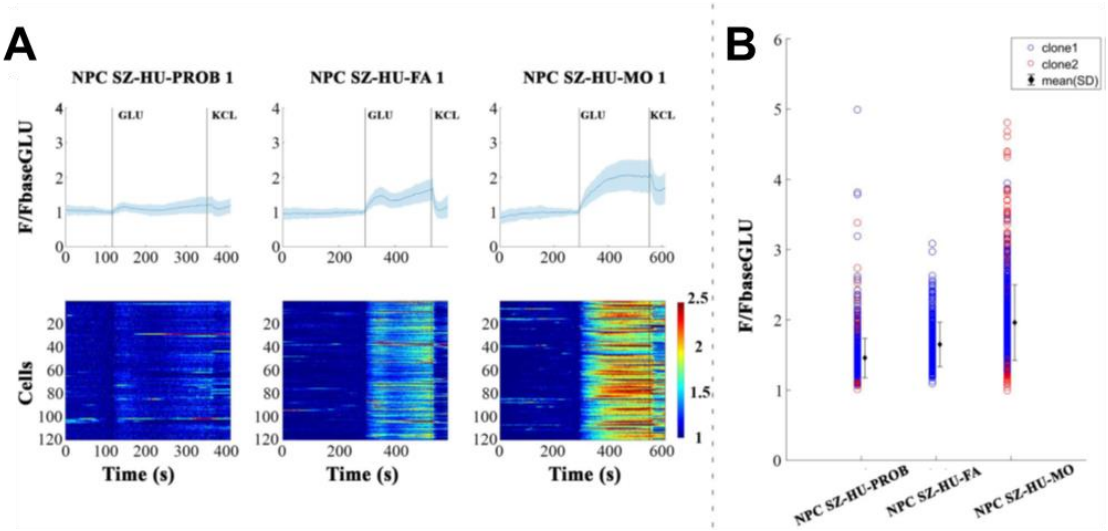

Figure 23. *Exploration of calcium activity in hippocampal NPCs A) Normalized Calcium activity (F/FbaseGlu) is depicted for one representative measurement of NPCs from each subject. The upper part of the subplot displays the mean activity (+/- standard deviation, depicted in shattered blue) on the Y-axis against time on the X-axis. The lower part illustrates the activity of all cells over time, with color indicating Calcium activity. B) Each circle represents the normalized Calcium activity of one cell for each subject in each clone (N = 3 independent experiments, n = 200–250 cells/experiment). Black diamonds represent the mean activity of a subject for both clones, with error bars indicating one standard deviation. Red circles depict NPCs derived from hiPSC clone one, while blue circles represent NPCs from hiPSC clone 2 (50).*

DOI:10.14753/SE.2025.3192

4.3 Summary of Results

These studies investigate the biological impact of two DNMs found in SCZ patients. Previously, de novo mutations in schizophrenic patients were identified, and two of them were selected for further experiments.

In the first project, a patient with a DNM in the gene *ZMYND11* was presented.

We created isogenic hiPSC lines, where the *ZMYND11* mutation was either corrected in patient-derived cells or introduced into control cells. These lines were differentiated into hippocampal NPCs and DGGCs, which were then subjected to detailed morphological, transcriptomic, and functional analyses.

The mutation did not affect the viability, growth capacity and visible morphological properties of the cells and cell cultures.

Transcriptomic profiling of the differentiated cells revealed significant changes in gene expression. In the mutant lines, there was a notable upregulation of genes associated with neuronal differentiation and a downregulation of genes involved in cell adhesion. This suggests that the ZMYND11 mutation alters neuronal differentiation.

Functionally, the mutant neurons exhibited decreased reactivity to glutamate, as demonstrated by calcium-imaging experiments. This reduced glutamate response was quantified and found to be significantly lower in mutant cells compared to wild-type controls.

In the second project involving a patient with 3 DNMs (*KHSRP, LRRC7 and KIRD1L2*) was presented.

In this project we decided to use a different experimental approach: we compared the cells of the patient to the cells of both their parents. Bulk RNA sequencing revealed transcriptional differences in the NPCs. GO and pathway analyses indicated that the differentially expressed genes were enriched in pathways critical to neuron formation, axon development, neurogenesis, Wnt signaling, and Calcium signaling.

Further phenotypic analysis using calcium imaging techniques showed significant functional differences in the NPCs' activity. The NPCs derived from the SCZ patient

DOI:10.14753/SE.2025.3192

demonstrated a significantly weaker response to glutamate compared to those from the unaffected parents.

The findings from both projects show that these DNMs impact neurodevelopmental processes and synaptic function in NPCs and DGGCs. Both mutations led to significant changes in gene expression and neuronal activity, suggesting a common pathway through which these genetic alterations might contribute to the pathophysiology of SCZ. By integrating results from more projects, we may get a broader perspective of the molecular mechanisms underlying SCZ.

Figure 24 below summarizes our hypothesis of possible cause and effect cascade, how a DNM at the DNA level may have slightly disrupted the delicate equilibrium of neurodevelopment. This disruption, along with many other factors, may contribute to a clinically observable imbalance of mental function that we call SCZ.

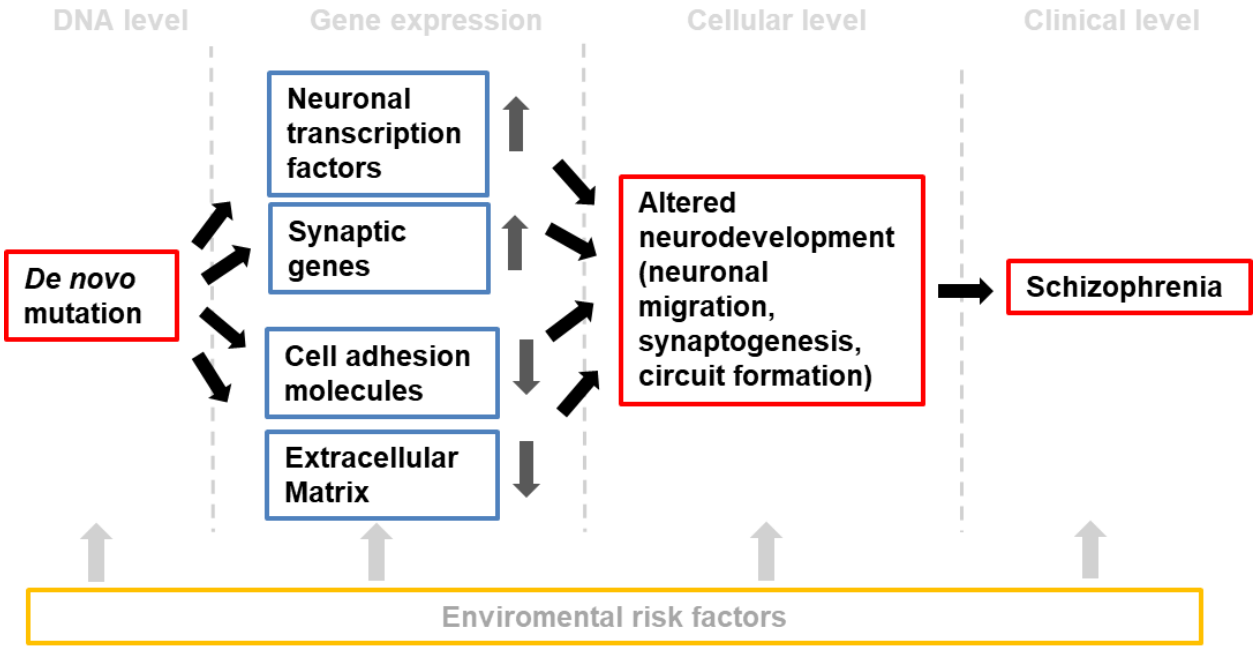

Figure 24. *Schematic summary of possible cause-effect relationships at different biological levels.*

DOI:10.14753/SE.2025.3192

5 Discussion

We presented a series of experiments aimed at identifying the biological effects of previously undescribed DNMs in SCZ patients: a nonsense mutation in the *ZMYND11* gene and missense mutations in the *KHSRP* and *LRRC7* genes.

Our main question was: How do these mutations affect neuronal development and function in humans? Using hiPSC-based disease models, we generated hippocampal NPCs and DGGCs from both patients to explore how these mutations affect neurodevelopment and function.

For the *ZMYND11* mutation, we found altered transcriptomic profiles, particularly in genes related to neuronal differentiation and synaptic function, as well as a reduced glutamate response in patient-derived neurons.

In the case carrying the *KHSRP* and *LRRC7* mutations, we observed molecular and functional phenotypes with notable differences between cell lines from the trio, which could be linked to neurodevelopmental pathology and, in part, to the identified DNMs. The observed cell-autonomous phenotypes align partly with previous hiPSC-based SCZ models, although some findings are more characteristic of autism spectrum disorder (ASD).

We used different techniques to create genetic controls for our experiments. In the case of *ZMYND11* mutation, we decided to use CRISPR genome editing to specifically modify the target gene. In the case of *KHSRP* mutation we established the healthy parent cell lines to use as genetic controls. The two approaches both have several advantages and drawbacks.

The **isogenic pair model** allows for precise control over genetic variables. This reduces the influence of unrelated genetic variations and ensures that observed phenotypic differences are attributable solely to the targeted mutation. However, CRISPR editing can introduce off-target effects, and the model may lack the complexity of naturally occurring genetic backgrounds, limiting its generalizability to broader patient populations.

In contrast, the **case-parent trio model** includes hiPSCs derived from a patient and both parents, allowing us to assess the influence of DNMs in the context of natural genetic variability within a family, where family members share genetic backgrounds partially.

This model offers the advantage of examining how unique combinations of inherited and new genetic variations contribute to disease phenotypes. However, the case-parent trio model is more susceptible to confounding effects from unrelated background genetic variations, which can make it challenging to isolate the impact of specific DNMs. Additionally, creating hiPSC lines from multiple family members is resource-intensive and may limit the number of clones per individual, which can affect experimental consistency. The results should be interpreted and compared in the light of these techniques' strengths and limitations.

5.1 Impact of DNMs on Neuronal Differentiation and Function

5.1.1 *ZMYND11* 1495C>T nonsense mutation

ZMYND11 gene has been previously implicated in tumorigenesis and syndromic intellectual disability due to its biological functions and known mutations (76, 77).

Its role in tumor formation, specifically, has been well-studied and is associated with a loss of co-repressor function for actively transcribed genes (78). Although a *ZMYND11* single nucleotide variant (SNV) has been observed in SCZ, numerous DNMs in *ZMYND11* have been linked to various forms of intellectual disability, with or without brain malformations (79). These mutations predominantly affect the Bromo and MYND domains of the protein, and to our knowledge, no prior studies have reported a mutation in the NLS region. According to the Varsome database and personal communications with Mario Benvenuto researcher in Foggia, Italy, this same mutation was found in a child attention-deficit/hyperactivity disorder and speech delay and his unaffected mother, suggesting it could be a transmitted SNV associated with milder neurodevelopmental phenotypes. Our hypothesis is that previously described mutations may cause more severe neurological alterations and clinical manifestations, such as syndromic intellectual disability, through deficient ZMYND11 transcriptional regulation during neurodevelopment.

It is plausible that the mutation investigated in this study affects the protein's nucleocytoplasmic transport, with no direct deficit in ZMYND11's co-repressor function.

Haploinsufficiency or dominant-negative effects, however, remain possibilities. The altered nucleocytoplasmic ratio of ZMYND11 between wild-type and mutated hiPSC lines (**Figure 12**) supports the involvement of nucleocytoplasmic trafficking.

In mouse primary cells, ZMYND11 has been shown to downregulate during *in vitro* neuronal differentiation. Furthermore, ZMYND11 overexpression inhibited neuronal differentiation and reduced neurite outgrowth, suggesting an inhibitory role (58). In our model, ZMYND11 mRNA levels were lower in mutant hippocampal NPCs and neurons, although an overall increase in mRNA levels was observed during neuronal differentiation. (**Figure 15**)

Using isogenic pairs, we found that the R399X mutation does not significantly affect DGGC differentiation; both the Pat-Mut and Ctrl-Mut hiPSC lines differentiated into functional hippocampal NPCs expressing SOX2 and Nestin . Upon further differentiation, all NPC lines reached a mature neuronal stage characterized by MAP2 and PROX1 expression, as well as spontaneous Ca-transients indicative of synaptic activity. Interestingly, we observed that in hippocampal NPCs and neurons, ZMYND11 was localized exclusively in the cytoplasm, suggesting sequestration from the nucleus during neuronal differentiation, similar to the related protein, ZMYND8 (80). To further investigate subtle gene expression differences, we conducted transcriptomics at the NPC and neuronal stages using RNA sequencing.

5.1.2 *KHSRP* 6416869C>A missense mutation

Similarly in the case of *KHSRP* and *LRRC7* mutants, all hiPSC lines were differentiated into homogeneous SOX2- and NESTIN-expressing neuronal progenitors, followed by MAP2- and PROX1-expressing functional dentate gyrus neurons, consistent with previous reports. qPCR analysis showed efficient neuronal differentiation, evidenced by the expression of neuronal markers NeuroD1, FOXG1, and PROX1 in the proband-derived NPCs and neuronal cultures. Notably, NeuroD1 mRNA levels were higher in the proband-derived NPCs than in those derived from the parents. While Yu et al. reported lower expression of neuronal markers in SCZ-derived neurons in a case-control study (37), our trio-based design revealed nearly equal marker expression across the case-parent

lines. The mature neurons differentiated from the NPCs were functional, as shown by spontaneous activity in Ca-imaging experiments, although direct neuronal comparisons were not performed, as our primary focus was the neuronal progenitor stage.

5.2 Transcriptomic analysis

It's important to note that as a result of the hippocampal differentiation protocol we used, the NPCs already show transcriptomic differences in contrast to cortical differentiation protocols (37). Notably, in both SCZ samples, certain genes responsible for neuronal differentiation were upregulated at the NPC stage. Additionally, in the mature neuronal stage of the *ZMYND11* mutant, genes associated with neuronal function were upregulated. This pattern may indicate accelerated neuronal differentiation. While our data only provide transcriptomic evidence for this hypothesis, others have observed this phenotype in cellular models, such as organoids (81). Overexpression of neuronal differentiation genes and underexpression of glial function genes is a molecular signature reported in other hiPSC models of SCZ (82). Precocious neuronal differentiation has also been observed in ASD, a genetically and clinically related condition (83). These findings further support the neurodevelopmental theory of SCZ and ASD (50).

Furthermore, in ZMYND11 mutant neurons, given the enrichment of GO terms related to synaptic function (e.g., "synapse organization" and "modulation of chemical synaptic transmission"), our study supports the hypothesis that synaptic dysfunction is a critical component of SCZ pathogenesis. Specifically, the enrichment of the GO term "synaptic transmission glutamatergic" points to the involvement of the glutamatergic system, as previously reported (84, 85). Overexpression of glutamate receptors is noteworthy, as numerous studies indicate that NMDAR hypofunction is a key aspect of SCZ pathophysiology at later stages (22). The discrepancy between overexpressed glutamatergic genes *in vitro* and *in vivo* glutamatergic hypofunction may reflect compensatory mechanisms or differences in developmental trajectories and different time points of the disease process.

In the ZMYND11 experiments, certain DE genes were observed in all samples (common across genetic backgrounds and differentiation stages), including some neuronal genes that could be promising candidates for further evaluation. Among the OE genes are LHX1

and LHX5, transcription factors crucial for forebrain and hippocampal development (86). The overexpression of *SHANK1*, a postsynaptic scaffold protein associated with glutamatergic transmission and ASD, and *ANO3*, a Ca-sensor implicated in synaptic responses in the hippocampus, further suggests a link between the *ZMYND11* mutation and synaptic dysfunction (87-89).

The presence of *KHDRBS2*, an RNA-binding protein involved in alternative splicing and linked to SCZ and Alzheimer's disease, in the OE group suggests that splicing dysregulation may underlie *ZMYND11* mutation effects (50, 90). Further studies could clarify how altered splicing contributes to this molecular phenotype. Underexpressed (UE) genes included *SLC34A2, CD74,* and *TPM2*. *SLC34A2*, with low but detectable brain expression, was previously identified as differentially expressed across SCZ, ASD, and bipolar disorder (91). The underexpression of *CD74*, predominantly expressed by glial cells, could suggest a decreased glia-neuron ratio in mutant samples (92). Single-cell RNA sequencing would be essential to confirm these findings.

The results from our RNA sequencing and functional assays from two SCZ patients with different genetic backgrounds suggest significant molecular differences in neurons derived from SCZ patients. Additionally, we would like to highlight the common features that indicate specific directions: namely, neuronal differentiation and synaptic function, especially in the glutamate system.

Our experiments did not include protein-level analyses, which are necessary to validate the significance of these transcriptomic changes. Nonetheless, the functional differences support that these DNMs have caused changes in cellular function.

5.3 Functional findings: reduced reactivity to glutamate

To assess functional differences, we conducted calcium imaging experiments. *In vivo*, Calcium signaling plays an essential role in the differentiation and migration of neural stem cell populations (93). Previous studies have shown that NPCs can be used to measure intracellular Calcium signaling, reflecting neuronal progenitors' reactivity to different ligands, with alterations seen in SCZ and ASD models (37). We tested NPC reactivity to glutamate, as dentate gyrus progenitors typically receive glutamatergic input.

KHSRP and *LRRC7* mutant proband-derived NPCs showed reduced calcium reactivity to glutamate compared to father- and mother-derived NPCs (74).

In another set of experiments, we tested the glutamate reactivity of DGGCs from *ZMYND11* mutant cells. Similarly to the NPCs, decreased activity was detected in the SCZ samples (34). Consistency between the two different SCZ cases further strengthens the role of the glutamate system in SCZ pathomechanism. Previous literature has shown similar findings: Yu et al. (45) reported lower spontaneous calcium activity in SCZ-derived neurons.

5.4 Synthesis of the results

Mutations in both *ZMYND11* and *KHSRP* appear to interfere with glutamatergic signaling, a pathway long associated with SCZ. Furthermore, the observed upregulation of neuronal differentiation genes with both mutations aligns with the neurodevelopmental hypothesis of SCZ, which posits that early disruptions in neuronal development can lead to lasting functional impairments in the brain (2).

The distinct mechanisms of these two mutations—ZMYND11 affecting transcriptional regulation via chromatin interactions, and KHSRP influencing RNA stability and splicing—highlight the range of molecular pathways that may contribute to SCZ. Based on this, it is worthwhile to study individual cases, as this could potentially lead to the development of more targeted, personalized treatment methods in the future. Additionally, the convergence of transcriptomic and functional phenotypes reinforces the idea that different biological pathways ultimately converge, and the clinical symptoms are caused by a dysfunction in a specific system, in this case, the glutamatergic synapses. This offers hope for further research, as we may find a pharmacological target that, when influenced, could potentially treat patients with diverse genetic backgrounds.

To our knowledge, this is the first study to employ reprogramming in a case-parent trio design to evaluate the potential molecular effects of DNMs in SCZ. Such studies may pave the way in the future for personalized, precision medicine approaches in hiPSC -based disease modeling.

5.5 Limitations

These findings should be considered within the study's strengths and limitations.

While hiPSC -based models are invaluable for examining specific mutations, they may not entirely reflect the complexity of *in vivo* neuronal development. The neurons derived *in vitro* resemble fetal neurons more closely, leaving open questions regarding how accurately they model the adult SCZ brain.

The XCL1 control cell line derived from a newborn's umbilical cord blood lacks data on long-term neuropsychiatric health, which, while not affecting *ZMYND11*-specific findings, may limit its appropriateness as a control.

In the *KHSRP* mutation where the case-parent trio approach was used, there is a bipolar patient in the investigated family who was not included in the experiments. This suggests that, in addition to the identified DNMs contributing to the disorder, the SCZ patient may also carry a significant level of genetic risk due to common variants.

Additionally, while CRISPR genome editing provides insights into underlying molecular pathways, its methodological limitations include off-target effects and the challenge of connecting transcriptomic changes in mutation-carrying NPCs and neurons to functional differences observed *in vivo*. Moreover, copy number variations potentially arising during the reprogramming process were not screened in the hiPSC lines.

Another limitation is the number of hiPSC clones used. While two hiPSC clones from the proband and the mother were examined, only one clone was available for the father, meaning the study did not fully meet the standard of using multiple clones per individual. However, the clones that were analyzed yielded consistent and comparable results.

Further studies will aim to support transcriptomic findings paired with measurable functional phenotypes, addressing the relevance of these physiological deficits to SCZ. Finally, as we focused on two patient-specific DNMs, these results may not generalize to other DNMs or other rare SCZ variants. Future studies should explore previously described SCZ DNMs and expand on ZMYND11's role in neurons and SCZ.

Future research should examine a wider range of mutations in larger SCZ patient cohorts, to determine whether these findings hold across different genetic variants.

DOI:10.14753/SE.2025.3192

Long term goal is to bridge these gaps, exploring how cellular dysfunction translates to mental health symptoms, and identifying specific molecular targets for pharmacological intervention.

Finally, investigating the interplay between genetic mutations and environmental factors may enhance our understanding of SCZ's multifactorial nature.

DOI:10.14753/SE.2025.3192

6 Conclusions

- **1. Neuronal Differentiation and characterization of hiPSC lines from SCZ samples**:
    - hiPSCs derived from SCZ patients can develop into hippocampal neuronal progenitors and functional DGGCs.
    - There were no significant observable differences in the differentiation, growth and morphology of neural progenitor cells (NPCs) and neurons (DGGCs) derived from SCZ patients.
    - Stage and fate specific markers were expressed similarly in patient-derived and control cells.
    - *ZMYND11* mutant hiPSCs show altered localisation of ZMYND11 protein
    - During neuronal differentiation, ZMYND11 protein becomes mostly cytoplasmatic.
- **2. Analysis of transcriptomic profiles of NPCs and neurons:**
    - RNA sequencing revealed significant changes in transcriptomic signatures of *ZMYND11* mutant progenitors and neurons
    - In *ZMYND11* mutant progenitors' genes responsible for neuronal differentiation were overexpressed. In ZMYND11 mutant neurons genes responsible for neuronal function and glutamatergic synaptic transmission were overexpressed
- **3. Functional Assessment of NPCs and Neurons:**
    - *KHSRP*, *LRRC7* mutant NPCs show decreased reaction to glutamate compared to parental cells.
    - DGGCs derived from *ZMYND11* mutant SCZ patient generate functional action potentials and calcium transients and respond to glutamate stimulation.
    - We observed reduced reaction of *ZMYND11* mutant DGGCs compared to isogenic controls.

DOI:10.14753/SE.2025.3192

7 Summary

In my PhD thesis, I explored *in vitro* disease modeling of schizophrenia (SCZ) through two patient-focused projects. Both SCZ patients carried unique de novo mutations: one in the ZMYND11 gene and another in the KHSRP and LRRC7 genes. Using induced pluripotent stem cell (hiPSC) technology, we investigated how these mutations influence neuronal differentiation and function.

We successfully reprogrammed patient cells into hiPSCs and established control lines through two methods: creating isogenic lines via CRISPR editing for the *ZMYND11* case and reprogramming parental cells for the KHSRP and LRRC7 case. These hiPSCs were differentiated into hippocampal neural progenitor cells (NPCs) and dentate gyrus granule cells (DGGCs) using a hippocampal differentiation protocol. Both SCZ and control lines formed functional NPCs and DGGCs, as evidenced by calcium transients and field potentials.

Transcriptomic analyses revealed significant differences in genes related to neuronal differentiation and synaptic function, indicating altered developmental pathways. Functional studies showed decreased glutamate reactivity in SCZ samples: in NPCs for KHSRP and LRRC7 mutations, and in DGGCs for ZMYND11 mutations.

Overall, our findings demonstrate that these mutations disrupt neuronal differentiation at the transcriptomic level and impair glutamatergic signaling at the functional level. These results support the neurodevelopmental theory of SCZ and highlight the role of glutamatergic neurotransmission and synaptic dysfunction in SCZ pathology. Our work identifies potential therapeutic targets and emphasizes the convergent molecular pathways underlying neuronal dysfunction in SCZ.

8 References

1. McGrath J, Saha S, Chant D, Welham J. Schizophrenia: a concise overview of incidence, prevalence, and mortality. Epidemiologic reviews. 2008;30:67-76.

2. Kahn RS, Sommer IE, Murray RM, Meyer-Lindenberg A, Weinberger DR, Cannon TD, et al. Schizophrenia. Nat Rev Dis Primers. 2015;1:15067.

3. Jauhar S, Johnstone M, McKenna PJ. Schizophrenia. Lancet (London, England). 2022;399(10323):473-86.

4. Howes DO, Murray MR. Schizophrenia: an integrated sociodevelopmental-cognitive model. The Lancet. 2014;383(9929):1677-87.

5. Murray MR, Lewis WS. Is schizophrenia a neurodevelopmental disorder? BMJ. 1987;295(6600):681-2.

6. Kahn RS, Sommer IE, Murray RM, Meyer-Lindenberg A, Weinberger DR, Cannon TD, et al. Schizophrenia. Nature Reviews Disease Primers. 2015;1(3):15067.

7. Réthelyi J, Benkovits J, Bitter I. Genes and environments in schizophrenia: The different pieces of a manifold puzzle. Neuroscience and biobehavioral reviews. 2013;37(10):2424-37.

8. Legge SE, Santoro ML, Periyasamy S, Okewole A, Arsalan A, Kowalec K. Genetic architecture of schizophrenia: a review of major advancements. Psychological medicine. 2021;51(13):2168-77.

9. Nakamura M, Takata A. Recent developments in schizophrenia genetics: Understanding the polygenic basis of the disease. Psychiatry and Clinical Neurosciences. 2023;77(3):101-11.

10. Fromer M, Pocklington AJ, Kavanagh DH, Williams HJ, Dwyer S, Gormley P, et al. De novo mutations in schizophrenia implicate synaptic networks. Nature. 2014;506(7487):179-84.

11. Zuk O, Hechter E, Sunyaev SR, Lander ES. The mystery of missing heritability: Genetic interactions create phantom heritability. Proceedings of the National Academy of Sciences of the United States of America. 2012;109(4):1193-8.

12. Singh T, Poterba T, Curtis D, Akil H, Al Eissa M, Barchas JD, et al. Rare coding variants in ten genes confer substantial risk for schizophrenia. Nature. 2022;604(7906):509-16.

13. Liu C, Jiang Y, Wang X, Ma H, Zhang Z, Han J. Genetic landscape of schizophrenia: A systematic review and meta-analysis of de novo mutations. Schizophrenia Bulletin. 2023;49(1):88-100.

14. Trubetskoy V, Pardiñas FA, Qi T, Panagiotaropoulou G, Awasthi S, Bigdeli BT, et al. Mapping genomic loci implicates genes and synaptic biology in schizophrenia. Nature. 2022;604(7906):502-8.

15. Balakrishna N, Curtis D. Exome sequencing and gene-based analysis confirm intellectual disability genes are involved in schizophrenia. Molecular psychiatry. 2020;25:2962-74.

16. Purcell SM, Wray NR, Stone JL, Visscher PM, O'Donovan MC, Sullivan PF, et al. Common polygenic variation contributes to risk of schizophrenia and bipolar disorder. Nature. 2009;460(7256):748-52.

17. Howes OD, Kapur S. The dopamine hypothesis of schizophrenia: version III--the final common pathway. Schizophr Bull. 2009;35(3):549-62.

18. Moncrieff J. A critique of the dopamine hypothesis of schizophrenia and psychosis. Harv Rev Psychiatry. 2009;17(3):214-25.

19. Birnbaum R, Weinberger DR. Genetic insights into the neurodevelopmental origins of schizophrenia. Nature Reviews Neuroscience. 2020;21:271-84.

20. Weinberger DR, Berman KF, Suddath R, Torrey EF. Evidence of dysfunction of a prefrontal-limbic network in schizophrenia: a magnetic resonance imaging and regional cerebral blood flow study of discordant monozygotic twins. The American journal of psychiatry. 1992;149(7):890-7.

21. Nakahara S, Matsumoto M, Erp VMGT. Hippocampal subregion abnormalities in schizophrenia: A systematic review of structural and physiological imaging studies. Neuropsychopharmacology Reports. 2018;38(4):156-66.

22. Coyle JT, Basu AC, Benneyworth MA, Balu DT, Konopaske GT. Glutamatergic synaptic dysregulation in schizophrenia: Therapeutic implications. Handbook of experimental pharmacology. 2012;NA(213):267-95.

23. Lodge DJ, Grace AA. Developmental pathology, dopamine, and stress: A model for the age of onset of schizophrenia symptoms. Schizophrenia Bulletin. 2011;37:480-5.

24. Harrison PJ. Postmortem studies in schizophrenia. Dialogues Clin Neurosci. 2000;2(4):349-57.

25. Weinberger DR, Radulescu E. Finding the elusive psychiatric "lesion" with 21st-century neuroanatomy: A note of caution. American Journal of Psychiatry. 2017;173:27-33.

26. Winship IR, Dursun SM, Baker GB, Balista PA, Kandratavicius L, Maia-de-Oliveira JP, et al. An Overview of Animal Models Related to Schizophrenia. The Canadian Journal of Psychiatry. 2019;64(1):5-17.

27. Takahashi K, Yamanaka S. Induction of pluripotent stem cells from mouse embryonic and adult fibroblast cultures by defined factors. Cell. 2006;126(4):663-76.

28. Brennand KJ, Simone A, Jou J, Gelboin-Burkhart C, Tran N, Sangar S, et al. Modelling schizophrenia using human induced pluripotent stem cells. Nature. 2011;473(7346):221-5.

29. Kiskinis E, Eggan K. Progress toward the clinical application of patient-specific pluripotent stem cells. Journal of Clinical Investigation. 2010;120:51-9.

30. Kathuria A, Lopez-Lengowski K, Jagtap S, McPhie DL, Tucker S, Karmacharya R. Transcriptomic deficiencies in synapse development in 3D cerebral organoids derived from schizophrenia patients. Molecular psychiatry. 2020;25:791-805.

31. Robicsek O, Karry R, Petit I, Salman-Kesner N, Muller FJ, Klein E, et al. Abnormal neuronal differentiation and mitochondrial dysfunction in hair follicle-derived induced pluripotent stem cells of schizophrenia patients. Molecular psychiatry. 2013;18(10):1067-76.

32. Moslem M, Ooi JK, Wichmann J, Zarrei M, Scherer SW. hiPSC-derived neurons and neural progenitors as a model for schizophrenia research. Molecular psychiatry. 2019;24:1677-92.

33. Rasanen N, Tiihonen J, Koskuvi M, Lehtonen S, Koistinaho J. The iPSC perspective on schizophrenia. Trends Neurosci. 2022;45(1):8-26.

34. Tordai C, Hathy E, Gyergyak H, Vincze K, Baradits M, Koller J, et al. Probing the biological consequences of a previously undescribed de novo mutation of ZMYND11 in a schizophrenia patient by CRISPR genome editing and induced pluripotent stem cell based in vitro disease-modeling. Schizophr Res. 2024.

35. Sarkar A, Mei A, Paquola ACM, Stern S, Bardy C, Klug JR, et al. Efficient Generation of CA3 Neurons from Human Pluripotent Stem Cells Enables Modeling of Hippocampal Connectivity In Vitro. Cell stem cell. 2018;22(5):684-97.e9.

36. Dubonyte U, Asenjo-Martinez A, Werge T, Lage K, Kirkeby A. Current advancements of modelling schizophrenia using patient-derived induced pluripotent stem cells. Acta neuropathologica communications. 2022;10(1):183-NA.

37. Yu DX, Di Giorgio FP, Yao J, Marchetto MC, Brennand K, Wright R, et al. Modeling hippocampal neurogenesis using human pluripotent stem cells. Stem cell reports. 2014;2(3):295-310.

38. Han J, Kim HJ, Schafer ST, Paquola A, Clemenson GD, Toda T, et al. Functional Implications of miR-19 in the Migration of Newborn Neurons in the Adult Brain. Neuron. 2016;91(1):79-89.

39. Lieberman JA, Girgis RR, Brucato G, Moore H, Provenzano F, Kegeles L, et al. Hippocampal dysfunction in the pathophysiology of schizophrenia: a selective review and hypothesis for early detection and intervention. Molecular psychiatry. 2018;23(8):1764-72.

40. Reif A, Fritzen S, Finger M, Strobel A, Lauer M, Schmitt A, et al. Neural stem cell proliferation is decreased in schizophrenia, but not in depression. Molecular psychiatry. 2006;11(5):514-22.

41. Steen RG, Mull C, McClure R, Hamer RM, Lieberman JA. Brain volume in first-episode schizophrenia: systematic review and meta-analysis of magnetic resonance

imaging studies. The British journal of psychiatry : the journal of mental science. 2006;188:510-8.

42. Walton NM, Zhou Y, Kogan JH, Shin R, Webster M, Gross AK, et al. Detection of an immature dentate gyrus feature in human schizophrenia/bipolar patients. Transl Psychiatry. 2012;2(7):e135.

43. Dhikav V, Anand KS. Is hippocampal atrophy a future drug target? Med Hypotheses. 2007;68(6):1300-6.

44. Kang E, Wen Z, Song H, Christian KM, Ming GL. Adult Neurogenesis and Psychiatric Disorders. Cold Spring Harb Perspect Biol. 2016;8(9).

45. Yu DX, Di Giorgio FP, Yao J, Marchetto MC, Brennand KJ, Wright R, et al. Modeling Hippocampal Neurogenesis Using Human Pluripotent Stem Cells. Stem cell reports. 2014;2(3):295-310.

46. Konstantinides N, Desplan C. Neuronal differentiation strategies: insights from single-cell sequencing and machine learning. Development. 2020;147(23).

47. Huch M, Knoblich JA, Lutolf MP, Martinez-Arias A. The hope and the hype of organoid research. Development. 2017;144(6):938-41.

48. Liang G, Zhang Y. Genetic and epigenetic variations in iPSCs: potential causes and implications for application. Cell Stem Cell. 2013;13(2):149-59.

49. Srikanth P, Han K, Callahan DG, Makovkina E, Muratore CR, Lalli MA, et al. Genomic DISC1 Disruption in hiPSCs Alters Wnt Signaling and Neural Cell Fate. Cell Rep. 2015;12(9):1414-29.

50. Hathy E, Szabo E, Varga N, Erdei Z, Tordai C, Czehlar B, et al. Investigation of de novo mutations in a schizophrenia case-parent trio by induced pluripotent stem cell-based in vitro disease modeling: convergence of schizophrenia- and autism-related cellular phenotypes. Stem Cell Res Ther. 2020;11(1):504.

51. Pulay AJ, Koller J, Horváth A, Balicza P, Benkovits J, Zahuczky G, et al. Functional gene clusters and pathway associations in schizophrenia: result from a whole-exome sequencing study. European Neuropsychopharmacology. 2016;26(NA):S184-NA.

52. Moskowitz AM, Belnap N, Siniard AL, Szelinger S, Claasen AM, Richholt RF, et al. A de novo missense mutation in ZMYND11 is associated with global developmental delay, seizures, and hypotonia. Cold Spring Harb Mol Case Stud. 2016;2(5):a000851.

53. Tiihonen J, Koskuvi M, Lähteenvuo M, Trontti K, Ojansuu I, Vaurio O, et al. Molecular signaling pathways underlying schizophrenia. Schizophr Res. 2021;232:33-41.

54. Wang J, Qin S, Li F, Li S, Zhang W, Peng J, et al. Crystal structure of human BS69 Bromo-ZnF-PWWP reveals its role in H3K36me3 nucleosome binding. Cell research. 2014;24(7):890-3.

55. Kopanos C, Tsiolkas V, Kouris A, Chapple CE, Albarca Aguilera M, Meyer R, et al. VarSome: the human genomic variant search engine. Bioinformatics. 2019;35(11):1978-80.

56. Yu H, Hou Y, Liu G, Song Y, Chen S, Huang S, et al. Expression of ZMYND11 in various human tissues. Gene. 2009;429:16-20.

57. Wen H, Li Y, Xi Y, Jiang S, Stratton SA, Peng D, et al. ZMYND11 links histone H3.3K36me3 to transcription elongation and tumour suppression. Nature. 2014;508(7495):263-8.

58. Yu B, Shao Y, Zhang C, Chen Y, Zhong Q, Zhang J, et al. BS69 undergoes SUMO modification and plays an inhibitory role in muscle and neuronal differentiation. Exp Cell Res. 2009;315(20):3543-53.

59. Hathy E, Szabo E, Vincze K, Haltrich I, Kiss E, Varga N, et al. Generation of multiple iPSC clones from a male schizophrenia patient carrying de novo mutations in genes KHSRP, LRRC7, and KIR2DL1, and his parents. Stem Cell Res. 2021;51:102140.

60. Briata P, Bordo D, Puppo M, Gorlero F, Rossi M, Perrone-Bizzozero N, et al. Diverse roles of the nucleic acid-binding protein KHSRP in cell differentiation and disease. Wiley Interdiscip Rev RNA. 2016;7(2):227-40.

61. Patel P, Buchanan CN, Zdradzinski MD, Sahoo PK, Kar AN, Lee SJ, et al. Intra-axonal translation of Khsrp mRNA slows axon regeneration by destabilizing localized mRNAs. Nucleic Acids Res. 2022;50(10):5772-92.

62. Perrone-Bizzozero N. Neuropsychiatric Implications Of RNA-Binding Proteins HuD And KSRP Revealed By Genome-Wide Identification Of Their Targets. European Neuropsychopharmacology. 2019;29:S721.

63. Olguin SL, Patel P, Buchanan CN, Dell'Orco M, Gardiner AS, Cole R, et al. KHSRP loss increases neuronal growth and synaptic transmission and alters memory consolidation through RNA stabilization. Communications Biology. 2022;5(1):672.

64. Szabo G, Gonda X, Bakos N, Karadi K, Benko Z. KHSRP as a potential genetic risk factor for schizophrenia: Evidence from transcriptomic analysis. Neuroscience. 2019;400:112-23.

65. Grant SG, Marshall MC, Mintz IM, Curzon P, Berg DK, Oppenheim RW. LRRC7 (densin-180) knockout mouse as a model of neurodevelopmental disorders. The Journal of Neuroscience. 2017;37:7235-46.

66. Fan QR, Long EO, Wiley DC. Crystal structure of the human natural killer cell inhibitory receptor KIR2DL1-HLA-Cw4 complex. Nat Immunol. 2001;2(5):452-60.

67. Hathy EM. Szkizofrénia in vitro betegségmodellezése indukált pluripotens őssejt alapú rendszerrel.

68. Erdei Z, Lőrincz R, Szebényi K, Péntek A, Varga N, Likó I, et al. Expression pattern of the human ABC transporters in pluripotent embryonic stem cells and in their derivatives. Cytometry Part B: Clinical Cytometry. 2014;NA(NA):n/a-n/a.

69. Péntek A, Pászty K, Apáti Á. Analysis of Intracellular Calcium Signaling in Human Embryonic Stem Cells. Methods in molecular biology (Clifton, NJ). 2014;1307(NA):141-7.

70. Kim D, Paggi JM, Park C, Bennett C, Salzberg SL. Graph-based genome alignment and genotyping with HISAT2 and HISAT-genotype. Nature biotechnology. 2019;37(8):907-15.

71. Love MI, Huber W, Anders S. Moderated estimation of fold change and dispersion for RNA-seq data with DESeq2. Genome biology. 2014;15(12):002832-550.

72. Koopmans F, van Nierop P, Andres-Alonso M, Byrnes A, Cijsouw T, Coba MP, et al. SynGO : An Evidence-Based, Expert-Curated Knowledge Base for the Synapse. Neuron. 2019;103(2):217-34.

73. Luo W, Pant G, Bhavnasi YK, Blanchard SG, Jr, Brouwer C. Pathview Web: user friendly pathway visualization and data integration. Nucleic Acids Research. 2017;45(W1):W501-W8.

74. Hathy E, Szabó E, Varga N, Erdei Z, Tordai C, Czehlár B, et al. Investigation of de novo mutations in a schizophrenia case-parent trio by induced pluripotent stem cell-based in vitro disease modeling: convergence of schizophrenia- and autism-related cellular phenotypes. Stem cell research & therapy. 2020;11(1):504-.

75. Vofely G, Berecz T, Szabo E, Szebenyi K, Hathy E, Orban TI, et al. Characterization of calcium signals in human induced pluripotent stem cell-derived dentate gyrus neuronal progenitors and mature neurons, stably expressing an advanced calcium indicator protein. Molecular and cellular neurosciences. 2018;88:222-30.

76. De Braekeleer E, Auffret R, Douet-Guilbert N, Basinko A, Le Bris M-J, Morel F, et al. Recurrent translocation (10;17)(p15;q21) in acute poorly differentiated myeloid leukemia likely results in ZMYND11-MBTD1 fusion. Leukemia & lymphoma. 2013;55(5):1189-90.

77. Li J, Galbo PM, Gong W, Storey AJ, Tsai Y-H, Yu X, et al. ZMYND11-MBTD1 induces leukemogenesis through hijacking NuA4/TIP60 acetyltransferase complex and a PWWP-mediated chromatin association mechanism. Nature communications. 2021;12(1):1045-.

78. Chen Y, Tsai Y-H, Tseng S-H. Regulation of BS69 Expression in Cancers. Anticancer research. 2019;39(7):3347-51.

79. Coe BP, Witherspoon K, Rosenfeld JA, van Bon BWM, Silfhout ATV-v, Bosco P, et al. Refining analyses of copy number variation identifies specific genes associated with developmental delay. Nature genetics. 2014;46(10):1063-71.

80. Yao N, Li J, Liu H, Wan J, Liu W, Zhang M. The Structure of the ZMYND8/Drebrin Complex Suggests a Cytoplasmic Sequestering Mechanism of ZMYND8 by Drebrin. Structure (London, England : 1993). 2017;25(11):1657-66.e3.

81. Sawada T, Chater TE, Sasagawa Y, Yoshimura M, Fujimori-Tonou N, Tanaka K, et al. Developmental excitation-inhibition imbalance underlying psychoses revealed by single-cell analyses of discordant twins-derived cerebral organoids. Molecular psychiatry. 2020;25(11):2695-711.

82. Narla ST, Lee YW, Benson CA, Sarder P, Brennand KJ, Stachowiak EK, et al. Common developmental genome deprogramming in schizophrenia - Role of Integrative Nuclear FGFR1 Signaling (INFS). Schizophr Res. 2017;185:17-32.

83. Schafer ST, Paquola ACM, Stern S, Gosselin D, Ku M, Pena M, et al. Pathological priming causes developmental gene network heterochronicity in autistic subject-derived neurons. Nature neuroscience. 2019;22(2):243-55.

84. Coyle JT, Konopaske GT, Jiang Z. Understanding the role of glutamate in schizophrenia: A review of recent progress. Schizophrenia Research. 2012;13:243-52.

85. Egerton A, Grace AA, Stone JM, Bossong MG, Sand M, McGuire P. Glutamate in schizophrenia: Neurodevelopmental perspectives and drug development. Schizophrenia research. 2020;223(NA):59-70.

86. Lui NC, Tam Y, Gao C, Huang J-D, Wang CC, Jiang L, et al. Lhx1/5 control dendritogenesis and spine morphogenesis of Purkinje cells via regulation of Espin. Nature communications. 2017;8(1):15079-.

87. Jiang Y-h, Ehlers MD. Modeling autism by SHANK gene mutations in mice. Neuron. 2013;78(1):8-27.

88. Huang W, Xiao S, Huang F, Harfe BD, Jan YN, Jan LY. Calcium-Activated Chloride Channels (CaCCs) Regulate Action Potential and Synaptic Response in Hippocampal Neurons. Neuron. 2012;74(1):179-92.

89. Pedemonte N, Galietta LJV. Structure and Function of TMEM16 Proteins (Anoctamins). Physiological reviews. 2014;94(2):419-59.

90. Gusareva ES, Carrasquillo MM, Bellenguez C, Cuyvers E, Colon S, Graff-Radford NR, et al. Genome-wide association interaction analysis for Alzheimer's disease. Neurobiology of aging. 2014;35(11):2436-43.

91. Guan J, Cai JJ, Ji G, Sham PC. Commonality in dysregulated expression of gene sets in cortical brains of individuals with autism, schizophrenia, and bipolar disorder. Translational psychiatry. 2019;9(1):152-.

92. Xu J, Sun J, Chen J, Wang L, Li A, Helm M, et al. RNA-Seq analysis implicates dysregulation of the immune system in schizophrenia. BMC genomics. 2012;13(8):1-10.

93. Toth AB, Shum AK, Prakriya M. Regulation of neurogenesis by calcium signaling. Cell calcium. 2016;59(2-3):124-34.

9 Bibliography of the candidate's publications

Publications related to the thesis:

1. Tordai, Csongor; Hathy, Edit; Gyergyák, Hella; Vincze, Katalin; Baradits, Máté; Koller, Júlia; Póti, Ádám; Jezsó, Bálint; Homolya, László; Molnár, Mária Judit et al.

Probing the biological consequences of a previously undescribed de novo mutation of ZMYND11 in a schizophrenia patient by CRISPR genome editing and induced pluripotent stem cell based in vitro disease-modeling

SCHIZOPHRENIA RESEARCH (2024)
IF: 3,6

2. Hathy, Edit; Szabó, Eszter; Varga, Nóra; Erdei, Zsuzsa; Tordai, Csongor; Czehlár, Boróka; Baradits, Máté; Jezsó, Bálint; Koller, Júlia; Nagy, László et al.

Investigation of de novo mutations in a schizophrenia case-parent trio by induced pluripotent stem cell-based in vitro disease modeling: convergence of schizophrenia- and autism-related cellular phenotypes

STEM CELL RESEARCH & THERAPY (2020)
IF: 7,1

Publications not related to the thesis:

Bálint, Jezsó; Sára, Kálmán; Kiara, Gitta Farkas; Edit, Hathy; Katalin, Vincze; Dzsenifer, Kovács-Schoblocher; Julianna, Lilienberg; Csongor, Tordai; Zsófia, Nemoda; Homolya, László et al.

Haloperidol, Olanzapine, and Risperidone Induce Morphological Changes in an In Vitro Model of Human Hippocampal Neurogenesis

BIOMOLECULES (2024)

IF: 4,8

∑IF: 15,

DOI:10.14753/SE.2025.3192

10 Acknowledgements.

I would like to emphasize again that all the work presented was accomplished as a team effort. It would be impossible to apply such complex molecular biology techniques, cell culture, and genetic interventions alone. The nature of this work required a truly interdisciplinary approach and mindset, heavily relying on the diverse competencies and strengths of the team members.

I am grateful to my supervisors Ágota Apáti and János Réthelyi, for welcoming me into their team, guiding me into this field of science, and supporting me closely throughout my PhD years. I also thank them for their human approach towards me, the deep, sometimes philosophical conversations, and the meaningful interactions at conferences. I appreciate their kind and constructive feedback and the pleasant atmosphere that was ever-present in our research group.

The dual-group arrangement had a profound impact on my work. It brought countless benefits but also presented some challenges. Having two perspectives on every research question heightened my awareness of the complexity of nature and the intricacies of the problems we sought to address. As a PhD student, I had two mentors who provided unique advice and insights, offering double the support. While their differing working styles and approaches enriched my learning experience, this situation also made decision-making processes more complex and, at times, slower, as every major decision required discussions with both supervisors.

Overall, I am deeply grateful for the enriching and successful experience I had during my PhD years. I gained a profound understanding of molecular biology, the nature of cells, and the challenges of modeling complex human disorders. Moreover, I learned valuable lessons about life in general.

I would like to thank all those who initiated the projects and compiled the findings detailed in the 1.4 Previous Results section, especially Edit Hathy.

Thank you to Edit Hathy, Kata Vincze, and Bea Haraszti, from whom I learned the practical skills of cell culture. Additionally, I am grateful to Kata Vincze for the uncountable hours of shared work, experiment planning, and brainstorming sessions.

DOI:10.14753/SE.2025.3192

I thank the students who participated in the lab work: Kiara Farkas, and Kamilla Szűcs, Marci Széphalmi, Blanka Kerecsényi, Sanjar Khabibullaev, Szép Levente.

I thank Réka Gárdi for the exciting collaboration and developing an algorithm for better baseline calculation and detecting spontaneous calcium signals in neurons during calcium imaging experiments.

My thanks go to Máté Baradits for collaborating on the multi-electrode array measurement techniques, analysis, and interpretation.

I appreciate Ádám Póti for teaching me transcriptomic analysis and the numerous joint brainstorming sessions we had while developing the project.

I am grateful to Tünde Berecz for her assistance with statistical analysis and for teaching me the evaluation of calcium imaging.

Thank you to Bálint Jezsó for the shared brainstorming, collaborative thinking, and his genuine curiosity about what is truly happening within the cell.

I thank my parents for instilling in me a love for science, dedication, and an immense curiosity and openness towards the world.

To my friends and my wife, thank you for your emotional support during difficult experiments and the writing of my thesis.

I am also grateful to the Doctoral School of Semmelweis University for the scholarship and training programme.

Finally, I thank the Hungarian State and Richter Gedeon Plc. for funding the material aspects of our research and for supporting me with a scholarship throughout this journey.